Electronic Supplementary Material (ESI) for Journal of Materials Chemistry C.

Tuning the Emission and Triplet Exciton Utilization Mechanism of Pyrazine-Based Multi-Carbazole Emitters and their use in Organic Light-Emitting Diodes

Dongyang Chen,[a,c] Le Zhang, [a,b] Tomas Matulaitis,[a] David B. Cordes,[a] Alexandra M. Z. Slawin,[a] Xiao-Hong Zhang[c], Ifor D. W. Samuel*[b] and Eli Zysman-Colman*[a]

[a] Organic Semiconductor Centre, EaStCHEM School of Chemistry, University of St Andrews, St Andrews, Fife, UK, KY16 9ST, U.K.

[b] Organic Semiconductor Centre, SUPA, School of Physics and Astronomy, University of St Andrews, North Haugh, St Andrews, Fife KY16 9SS, U.K.

[c] Functional Nano & Soft Materials (FUNSOM), Soochow University, Suzhou, Jiangsu, 215123 China.

Table of Contents

Synthesis and Chemical Characterization

General Synthetic Procedures

All experiments were carried out with commercial solvents from Fisher Scientific Ltd, except where specifically mentioned. Commercially obtained chemicals were used as received. All manipulations were carried out under an inert atmosphere using standard Schlenk line techniques.

^{1}H NMR, and ^{13}C NMR were recorded at room temperature on a Bruker Avance spectrometer at 400 or 500 MHz and 101 or 126 MHz, respectively. ^{1}H NMR and ^{13}C NMR spectra were referenced to the residual solvent peaks ($CDCl_3$ = 7.26 ppm for ^{1}H NMR and 77.2 ppm for ^{13}C NMR, acetone-d_6 = 2.05 ppm for ^{1}H NMR and 206.7 and 29.9 ppm for ^{13}C NMR, d_6-DMSO = 2.50 ppm for ^{1}H NMR and 39.5 ppm for ^{13}C NMR). The following abbreviations have been used for multiplicity assignments: "d" for doublet, "t" for triplet, "m" for multiplet, "td" for triplet of doublets and "ddd" for doublet of doublet of doublets. Elemental analysis was measured by School of Chemistry, Edinburgh University. GCMS analysis was conducted using a Shimadzu QP2010SE GC-MS equipped with a Shimadzu SH-Rtx-1 column (30 m × 0.25 mm). Samples for high resolution mass spectrum (HRMS) were sent to School of Chemistry Mass Spectrometry Service in University of Leeds for analysis.

Tetrachloropyrazine (4ClPz)

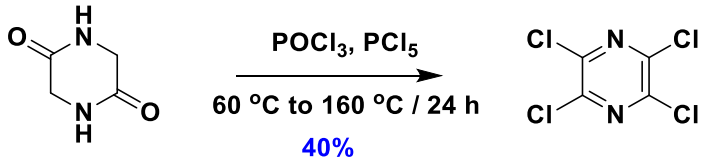

Synthesis of **4ClPz** was achieved by using a modified the literature procedure.[1] A mixture of 2,5-dioxopiperazine (1.1 g, 10 mmol, 1 equiv.) and phosphorus pentachloride (10.4 g, 50 mmol, 5 equiv.) were added to phosphorusoxychloride (30 mL, 50 mmol, 5 equiv.). The mixture was slowly heated up to 60 °C whereby a vigorous reaction was observed to occur. After removal of the volatile acid by distillation using a vigreux condenser (~ 1 h), the mixture was heated at 160 °C for 24 h. Upon cooling, the residue was dissolved in *n*-heptane and carefully added to icy water followed by extraction with DCM (3 × 50 mL). The combined organic layers were dried with anhydrous magnesium sulfate. The organic solvent was removed under reduced pressure and the crude product was purified by silica gel column chromatography. DCM/Hexane=1/10 was used as the eluent to afford **4ClPz** as a colorless solid.

Yield: 40%. **R_f**: 0.45 (10% DCM/Hexanes). **Mp**: 99-101 °C (Lit. Mp: 100 °C).[1] **^{13}C NMR (101MHz, $CDCl_3$) δ (ppm)**: 144.0; **LRMS** (GC-MS) **$[M]^+$ Calculated ($C_4Cl_4N_2$)**: 217.88; **Found**: 217.90, retention time: 4.64 min. The characterization matches that previously reported.[1]

2,3,5,6-tetra(9*H*-carbazol-9-yl)pyrazine (4CzPyz)

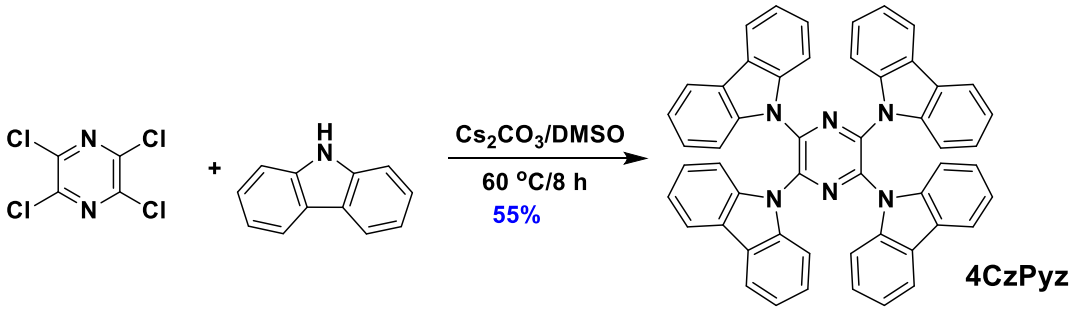

To a 250 mL flask were added **4ClPz** (210 mg, 1 mmol, 1 equiv.), carbazole (830 mg, 5 mmol, 5 equiv.), and cesium carbonate (1.6 g, 5 mmol, 5 quiv.). The flask was degassed by three cycles of vacuum-nitrogen purging and 20 mL of DMSO was injected. The mixture was stirred at 60 °C for 8 h under a nitrogen atmosphere. After cooling, the reaction mixture was poured into icy water followed by extraction with ethyl acetate (3 × 50 mL). The combined organic layers were dried with anhydrous magnesium sulfate. The organic solvent was removed under reduced pressure and the crude product was purified by silica gel column chromatography. DCM/Hexane=1/3 was used as eluent to afford **4CzPyz** as a light green solid.

Yield: 40%. **R_f**: 0.52 (40% DCM/Hexanes). **Mp**: over 410 °C. **^{1}H NMR (400 MHz, $CDCl_3$) δ (ppm)**: 7.89 – 7.85 (m, 8H), 7.55 (d, *J* = 8.2 Hz, 8H), 7.15 (ddd, *J* = 7.8, 7.2, 0.9 Hz, 8H), 7.02 (ddd, *J* = 8.4, 7.2, 1.3 Hz, 8H). **^{13}C NMR (101 MHz, $CDCl_3$) δ (ppm)**: 138.0, 135.4, 126.10, 124.5, 121.6, 119.8, 111.1. **HRMS** (ESI-MS) **$[M]^+$ Calculated: ($C_{52}H_{32}N_6$)** 741.2761; **Found**: 741.2736. **Elemental analysis**: **Calcd for $C_{52}H_{32}N_6$**: C, 84.30; H, 4.35; N, 11.34. **Found**: C, 84.60; H, 4.27; N, 11.11. **HPLC**: 5% H_2O/MeOH, 1.0 mL min^{-1}, 300 nm; tr (97.9 %) = 11.9 min. The characterization matches that previously reported.[2]

2-([1,1'-biphenyl]-2-yl)-3,5,6-trichloropyrazine (3ClBPz)

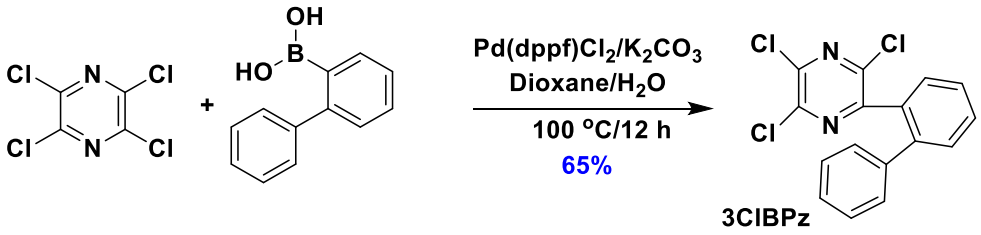

To a 250 mL flask were added **4ClPz** (210 mg, 1 mmol, 1 equiv.), [1,1'-biphenyl]-2-ylboronic acid (200 mg, 1 mmol, 1 equiv.), (1,1'-Bis(diphenylphosphino)ferrocene)palladium(II) dichloride (75 mg, 0.1 mmol, 0.1 equiv.), potassium carbonate (450 mg, 3 mmol, 3 equiv.). The flask was degassed by three cycles of vacuum-nitrogen purging and 2 mL of deionized water and 8 mL of dioxane were injected. The mixture was stirred at 100 °C for 12 h under a nitrogen atmosphere. After cooling, the reaction mixture was poured into icy water followed by extraction with DCM (3 × 50 mL). The combined organic layers were dried with anhydrous magnesium sulfate. The organic solvent was removed under reduced pressure and the crude product was purified by silica gel column chromatography. DCM/Hexane=1/4 was used as the eluent to afford **3ClBPz** as a white solid.

Yield: 65%. **R_f**: 0.62 (20% DCM/Hex). **Mp**: 150 °C. **^{1}H NMR (500 MHz, $CDCl_3$) δ (ppm)**: 7.64 – 7.57 (m, 1H), 7.55 – 7.46 (m, 3H), 7.29 (d, *J* = 2.4 Hz, 3H), 7.18 – 7.10 (m, 2H). **^{13}C NMR (126 MHz, $CDCl_3$)**

δ (ppm): 152.6, 144.4, 144.3, 143.8, 141.8, 140.0, 133.1, 130.3, 130.3, 130.0, 129.2, 128.4, 127.5, 127.5. **LRMS** (GC-MS) **$[M+H]^+$ Calculated: ($C_{16}H_9Cl_3N_2$)** 333.98; **Found**: 334.10, retention time: 9.10 min.

9,9',9''-(6-([1,1'-biphenyl]-2-yl)pyrazine-2,3,5-triyl)tris(9H-carbazole) (3CzBPz)

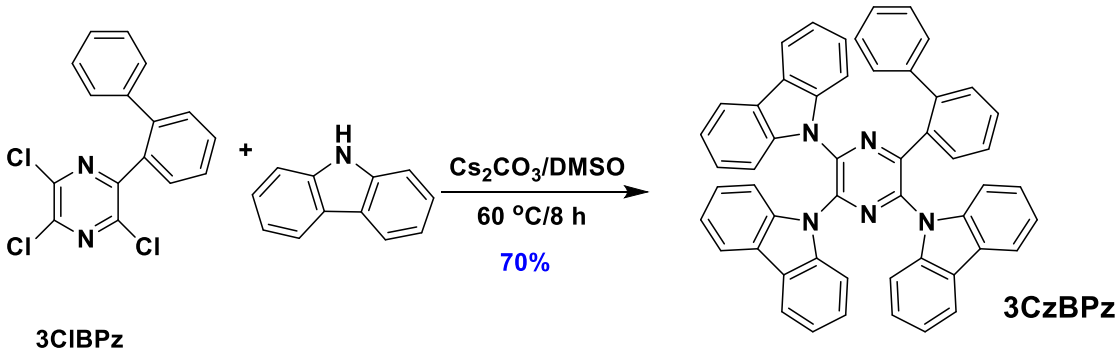

3ClBPz

To a 250 mL flask were added **3ClBPz** (330 mg, 1 mmol, 1 equiv.), carbazole (660 mg, 4 mmol, 4 equiv.), and cesium carbonate (1.3 g, 4 mmol, 4 equiv.). The flask was degassed by three cycles of vacuum-nitrogen purging and 20 mL of DMSO was injected. The mixture was stirred at 60 °C for 8 h under a nitrogen atmosphere. After cooling, the reaction mixture was poured into icy water followed by extraction with ethyl acetate (3 × 50 mL). The combined organic layers were dried with anhydrous magnesium sulfate. The organic solvent was removed under reduced pressure and the crude product was purified by silica gel column chromatography. DCM/Hexane=1/3 was used as the eluent to afford **3CzBPz** as a light-yellow solid.

Yield: 70%. **R_f**: 0.42 (30% DCM/Hexanes). **Mp**: 400 °C. **^{1}H NMR (400 MHz, Acetone-d_6) δ (ppm)**: 8.29 – 8.20 (m, 1H), 8.05 (d, J = 7.7 Hz, 2H), 8.01 – 7.87 (m, 4H), 7.55 (td, *J* = 7.6, 1.3 Hz, 5H), 7.37 (td, *J* = 7.6, 1.4 Hz, 1H), 7.25 – 6.99 (m, 15H), 6.94 – 6.78 (m, 3H), 6.72 – 6.56 (m, 2H). **^{13}C NMR (101 MHz, Acetone-d_6) δ (ppm)**: 148.6, 142.6, 140.4, 139.4, 139.3, 138.7, 138.4, 134.7, 132.4, 130.2, 128.5, 128.1, 128.0, 126.5, 125.9, 124.0, 121.8, 121.3, 120.7, 120.1, 111.4. **HRMS** (ESI-MS) **$[M+H]^+$ Calculated: ($C_{52}H_{34}N_5$)** 728.2809; **Found**: 728.2804. **Elemental analysis**: **Calcd for $C_{52}H_{33}N_5$**: C, 85.81; H, 4.57; N, 9.62. **Found**: C, 85.60; H, 4.66; N, 9.46. **HPLC**: 2% H_2O/MeOH, 1.0 mL min^{-1}, 300 nm; tr (97.9 %) = 4.0 min.

9,9'-(3,6-dichloropyrazine-2,5-diyl)bis(9H-carbazole) (2Cz2ClPz)

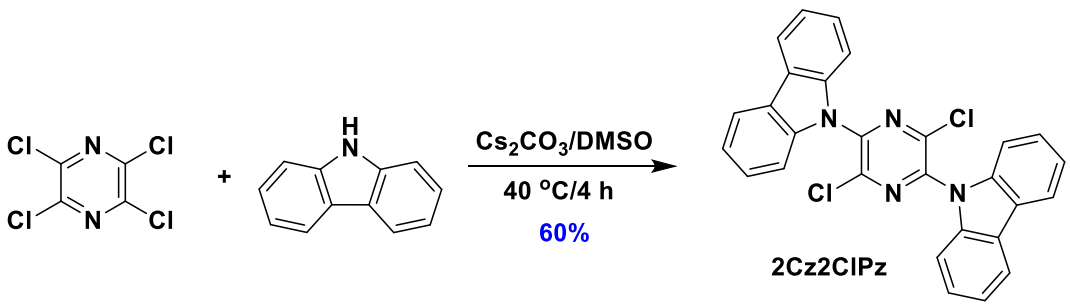

2Cz2ClPz

To a 250 mL flask were added **4ClPz** (210 mg, 1 mmol, 1 equiv.), carbazole (130 mg, 2 mmol, 2 equiv.), and cesium carbonate (640 g, 2 mmol, 2 equiv.). The flask was degassed by three cycles of vacuum-nitrogen purging and 20 mL of DMSO was injected. The mixture was stirred at 40 °C for 8 h under a nitrogen atmosphere. After cooling, the reaction mixture was poured into icy water followed by extraction with ether acetate (3 × 50 mL). The combined organic layers were dried with anhydrous magnesium sulfate. The organic solvent was removed under reduced pressure and the crude product was purified by silica gel column chromatography. DCM/Hexane=1/3 was used as the eluent to afford **2Cz2ClPz** as a light green solid.

Yield: 60%. **R_f**: 0.42 (40% DCM/Hex). **Mp**: 250 °C. **^{1}H NMR (400 MHz, $CDCl_3$) δ (ppm)**: 8.22 – 8.17 (m, 1H), 7.58 – 7.50 (m, 3H), 7.48 – 7.39 (m, 1H). **^{13}C NMR (101 MHz, $CDCl_3$) δ (ppm)**: 142.6, 138.0, 135.2, 125.9, 124.5, 121.6, 119.8, 111.1. **LRMS** (GC-MS) **$[M+H]^+$ Calculated: ($C_{28}H_{17}Cl_2N_4$)** 479.08; **Found**: 479.19, retention time: 18.56 min.

9,9'-(3,6-di([1,1'-biphenyl]-2-yl)pyrazine-2,5-diyl)bis(9H-carbazole) (2CzBPz)

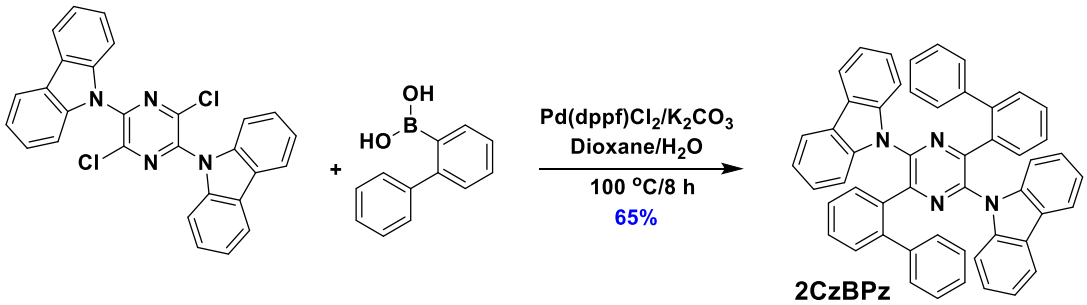

To a 250 mL flask were added **2Cz2ClPz** (480 mg, 1 mmol, 1 equiv.), [1,1'-biphenyl]-2-ylboronic acid (600 mg, 3 mmol, 3 equiv.), (1,1'-bis(diphenylphosphino)ferrocene)palladium(II) dichloride (75 mg, 0.1 mmol, 0.1 equiv.), potassium carbonate (1.3 g, 9 mmol, 9 equiv.). The flask was degassed by three cycles of vacuum-nitrogen purging and 2 mL of deionized water and 8 mL of dioxane were injected. The mixture was stirred at 100 °C for 12 h under a nitrogen atmosphere. After cooling, the reaction mixture was poured into icy water followed by extraction with DCM (3 × 50 mL). The combined organic layers were dried with anhydrous magnesium sulfate. The organic solvent was removed under reduced pressure and the crude product was purified by silica gel column chromatography. DCM/Hexane=1/4 was used as the eluent to afford **2CzBPz** as a white solid.

Yield: 65%. **R_f**: 0.44 (20% DCM/Hexanes). **Mp**: 395-398 °C. **^{1}H NMR (400 MHz, *d_6*-DMSO) δ (ppm)**: 8.08 (d, *J* = 7.6 Hz, 4H), 8.04 – 7.93 (m, 2H), 7.46 (td, *J* = 7.6, 1.2 Hz, 2H), 7.31 (td, *J* = 7.6, 1.4 Hz, 2H), 7.16 (t, *J* = 7.5 Hz, 4H), 7.03 (t, *J* = 7.7 Hz, 4H), 7.00 – 6.86 (m, 12H), 6.48 (d, *J* = 7.0 Hz, 4H). **^{13}C NMR (101 MHz, *d_6*-DMSO) δ (ppm)**: 148.6, 142.6, 140.4, 139.3, 138.7, 134.7, 132.4, 130.3, 128.5, 128.1, 125.8, 121.8, 121.3, 120.7, 111.4. **HRMS** (ESI-MS) **$[M+H]^+$ Calculated: ($C_{52}H_{35}N_4$)** 715.2844; **Found**: 715.2856. **Elemental analysis**: **Calcd for $C_{52}H_{34}N_4$**: C, 87.37; H, 4.79; N, 7.84. **Found**: C, 87.54; H, 4.89; N, 7.78. **HPLC**: 2% H_2O/MeOH, 1.0 mL min^{-1}, 300 nm; tr (98.5 %) = 4.8 min.

Theoretical Calculations

Ground state optimizations were carried out using Density Functional Theory (DFT) employing the PBE0[3]

functional with the Pople[4] 6-31G(d,p) basis set in vacuum, followed by frequency calculations at the same level of theory to ensure that an energy minimum were reached. Excited-state calculations and optimazations were performed employing the Tamm-Dancoff approximation (TDA)[5,6] to Time-Dependent DFT (TD-DFT) using the same functional and basis set for ground states and excited states geometry optimization. The spin-orbital coupling matrix element (SOCME) values between excited states were obtained by PySOC calculation based on optimized triplet states' geometry.[7] Gaussian09[8] software was employed for the calculations,[9] and GaussYiew 5.0 was used for visualization.[10]

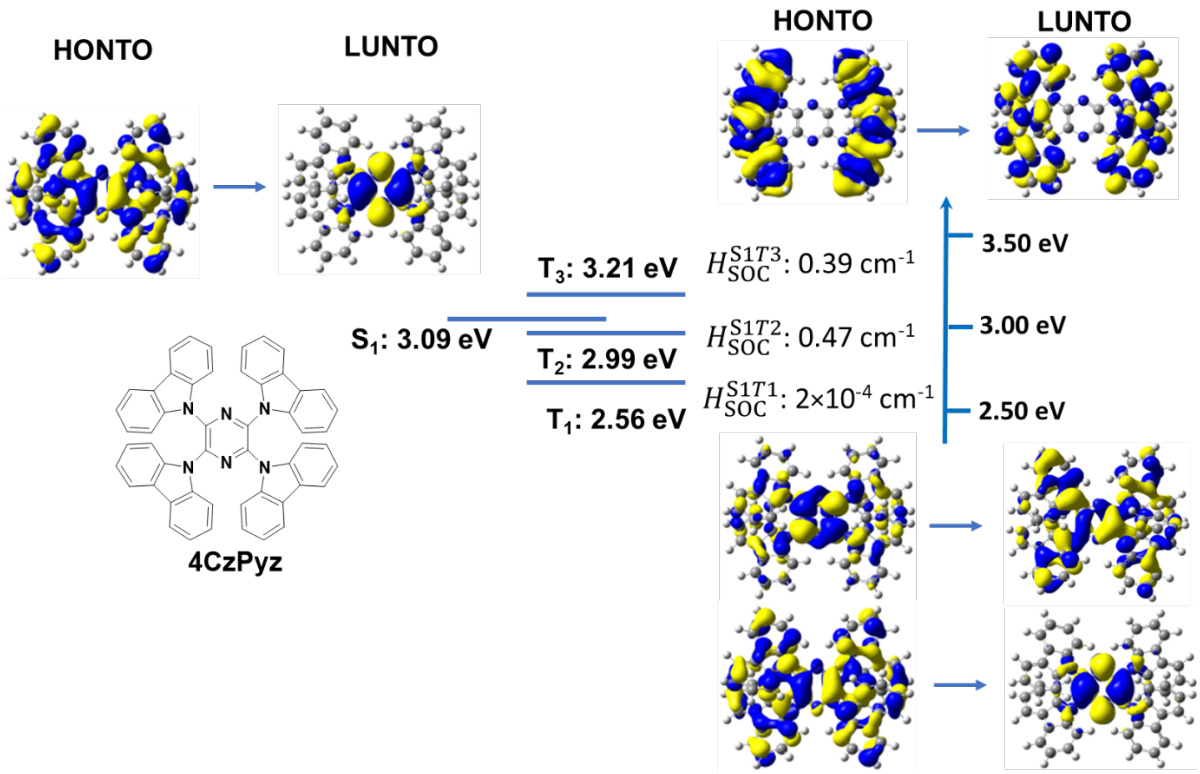

Figure **S1**. Natural transition orbitals analysis of excited states for **4CzPyz**.

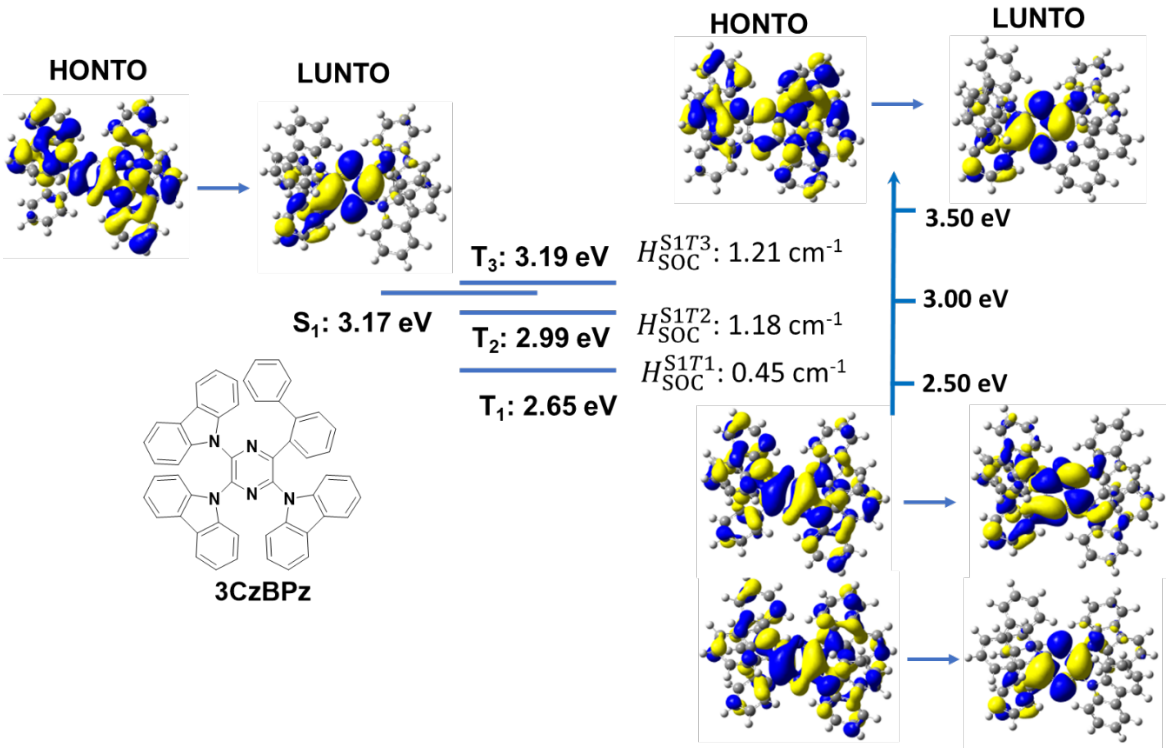

Figure **S2**. Natural transition orbitals analysis of excited states for **3CzBPz**.

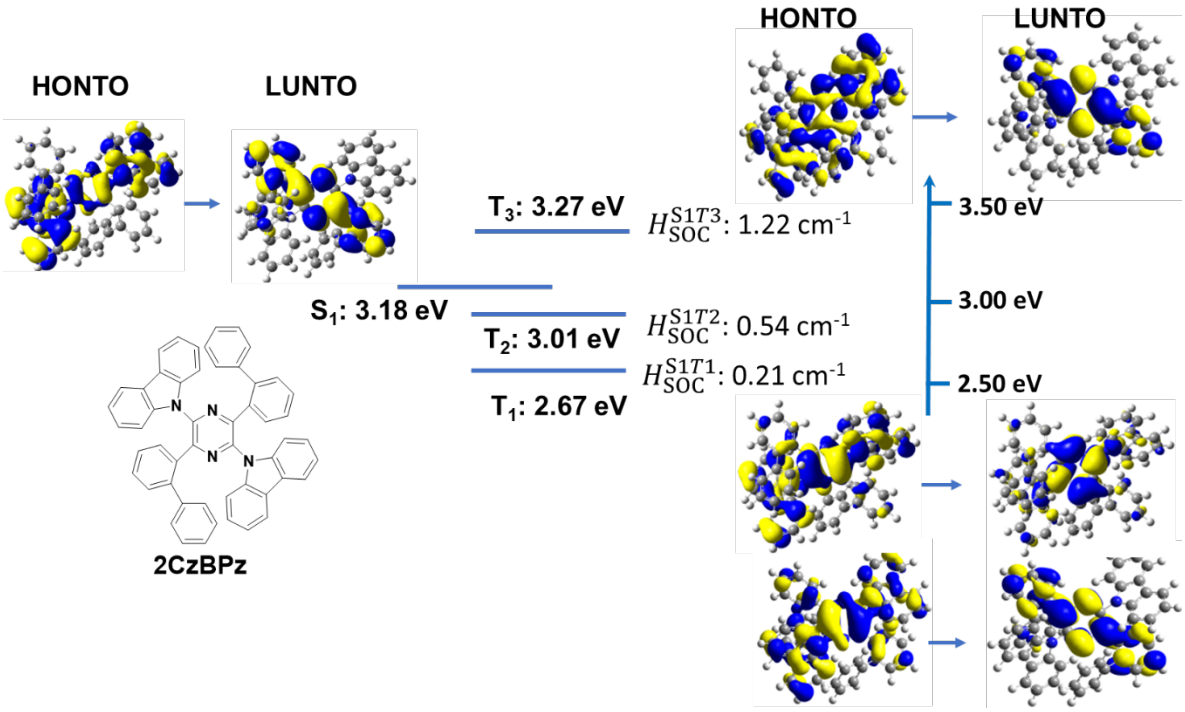

Figure **S3**. Natural transition orbitals analysis of excited states for **2CzBPz**.

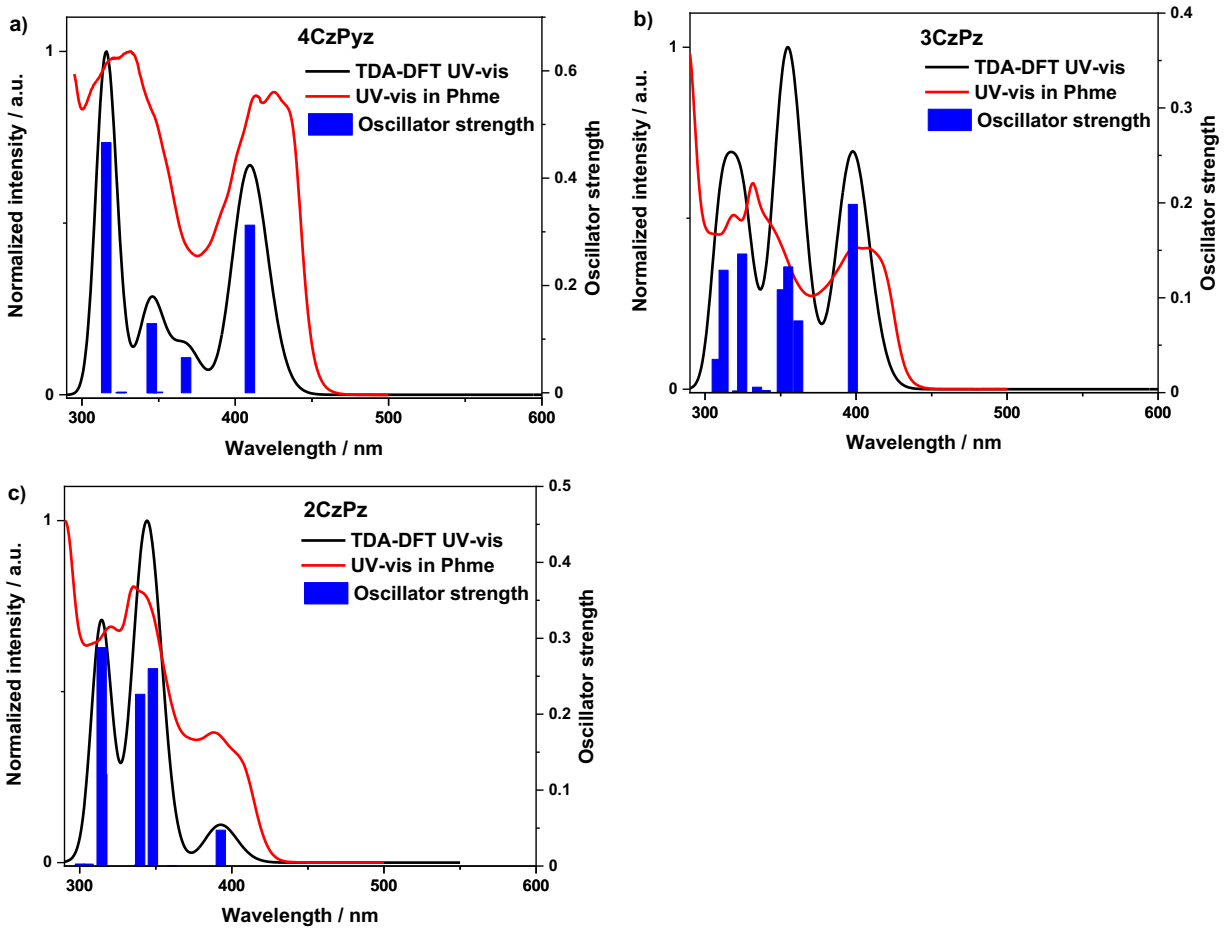

Figure **S4**. Calculated and experimental (in toluene) UV-*vis* absorption spectra and oscillator strength for a) **4CzPyz**, b) **3CzBPz**, and c) **2CzBPz**.

Photophysical measurements

Optically dilute solutions of concentrations in the order of 10^{-5} or 10^{-6} M were prepared in HPLC grade solvent for absorption and emission analysis. Absorption spectra were recorded at room temperature on a Shimadzu UV-1800 double beam spectrophotometer. Molar absorptivity values were determined from at least four solutions followed by linear regression analysis. Aerated solutions were bubbled with compressed air for 5 minutes whereas degassed solutions were prepared via five freeze-pump-thaw cycles prior to emission analysis using an in-house adapted fluorescence cuvette, itself purchased from Starna. Steady-state emission and excitation spectra and time-resolved emission spectra were recorded at 298 K using an Edinburgh Instruments FLS980 fluorimeter. Samples were excited at 340 nm for steady-state measurements and at 378 nm for time-resolved measurements Photoluminescence quantum yields for solutions were determined using the optically dilute method[11] in which four sample solutions with absorbances of ca. 0.10, 0.075, 0.050 and 0.025 at 360 nm were used. The Beer-Lambert law was found to remain linear at the concentrations of the solutions. For each sample, linearity between absorption and emission intensity was verified through linear regression analysis with the Pearson regression factor (R^2) for the linear fit of the data set surpassing 0.9. Individual relative quantum yield values were calculated for each solution and the values reported represent the slope obtained from the linear fit of these results. The quantum yield of the sample, Φ_{PL}, can be determined by the equation $\Phi_{PL} = (\Phi_r * \frac{A_r}{A_s} * \frac{I_s}{I_r} * \frac{n_s^2}{n_r^2})$,[11] where A stands for the

absorbance at the excitation wavelength (λ_{exc}: 360 nm), I is the integrated area under the corrected emission curve and n is the refractive index of the solvent with the subscripts "s" and "r" representing sample and reference respectively. Φ_r is the absolute quantum yield of the external reference quinine sulfate (Φ_r = 54.6% in 1 *N* H_2SO_4).[12] The experimental uncertainty in the emission quantum yields is conservatively estimated to be 10%, though we have found that statistically we can reproduce Φ_{PL}s to 3% relative error.

To prepare the 10 wt% doped films of emitters in a host matrix, 90% w/w (90 mg) of host was dissolved in 1 mL of solvent and to this, 10% w/w (10 mg) of emitter was added. Thin films were then spin-coated on a quartz substrate using a spin speed of 1500 rpm for 60 s to give a thickness of ~80 nm. Time-resolved decay curves for prompt fluorescence (100 ns time window) were measured using time correlated single photon counting (TCSPC) while time-resolved delayed fluorescence decays were measured using multi-channel scaling (MCS). The singlet-triplet splitting energy, ΔE_{ST} in the glass, was estimated from the onset of prompt fluorescence spectra and phosphorescence emission at 77 K. Phosphorescence spectra were measured from 1 ms after photoexcitation, with an iCCD exposure time was 9 ms. Prompt fluorescence spectra were measured from 1 ns after photoexcitation with an iCCD exposure time was 99 ns. The films were excited by a femtosecond laser emitting at 343 nm (Orpheus-N, model: SP-06-200-PP). Emission from the samples was focused onto a spectrograph (Chromex imaging, 250is spectrograph) and detected on a sensitive gated iCCD camera (Stanford Computer Optics, 4Picos) having sub-nanosecond resolution. Prompt fluorescence and phosphorescence in solid state were recorded on a Hitachi F-4600 fluorescence spectrophotometer with default collection intervals (delay: 1 ns, gate: 100 ns for fluorescence mode and delay: 2 ms, gate: 4 ms for phosphorescence mode). Photoluminescence quantum yield, Φ_{PL}, for solid films were measured using an integrating sphere in a Hamamatsu C9920-02 system with excitation at 330 nm under air and constant nitrogen gas flow.[13]

Electrochemistry measurements

Cyclic Voltammetry (CV) analysis was performed on an Electrochemical Analyzer potentiostat model 620E from CH Instruments at a sweep rate of 100 mV/s. Differential pulse voltammetry (DPV) was conducted with an increment potential of 0.004 V and a pulse amplitude, width, and period of 50 mV, 0.05, and 0.5 s, respectively. Samples were prepared as dichloromethane (DCM) solutions, which were degassed by sparging with DCM-saturated nitrogen gas for 20 minutes prior to measurements. All measurements were performed using 0.1 M DCM solution of tetra-*n*-butylammonium hexafluorophosphate ([nBu$_4$N]PF$_6$]). An Ag/Ag$^+$ electrode was used as the reference electrode while a platinum electrode and a platinum wire were used as the working electrode and counter electrode, respectively. The redox potentials are reported relative to a saturated calomel electrode (SCE) with a ferrocene/ferrocenium (Fc/Fc$^+$) redox couple as the internal standard (0.46 V vs SCE).[14]

X-Ray crystallography

X-ray diffraction data were collected either at 173 K using a Rigaku FR-X Ultrahigh brilliance Microfocus RA generator/confocal optics with XtaLAB P200 diffractometer [Mo Kα radiation (λ = 0.71075 Å)], or at 125 K using a Rigaku MM-007HF High Brilliance RA generator/confocal optics with XtaLAB P200 diffractometer [Cu Kα radiation (λ = 1.54187 Å)]. Intensity data were collected using ω-steps accumulating area detector images spanning at least a hemisphere of reciprocal space. Data for all compounds analysed were collected using CrystalClear[15] and processed (including correction for Lorentz, polarization and absorption) using either CrysAlisPro.[16] Structures were solved by direct (SIR2011)[17] or dual-space (SHELXT)[18] methods and refined by full-matrix least-squares against F^2 (SHELXL-2018/3).[19] Non-

hydrogen atoms were refined anisotropically, and hydrogen atoms were refined using a riding model. All crystals of **4CzPyz** were platy and showed a tendency for imperfect stacking of the plates. This resulted in both the apparent twinning in this sample and is also likely a cause of the elevated values of R_{int}, wR_2 and the maximum residual electron density. The structure of **2CzBPz** showed disorder in the orientation of the pendant phenyl of one biphenyl group, which were modelled across two sites. All calculations were performed using the Olex2 interface.[20] Selected crystallographic data are presented in Table **S1**. Deposition numbers 2280783-2280785 contains the supplementary crystallographic data for this paper. These data can be obtained free of charge from The Cambridge Crystallographic Data Centre via www.ccdc.cam.ac.uk/structures.

Table **S1**. Crystallographic data for **4CzPyz**, **3CzBPz**, and **2CzBPz**.

	4CzPyz	**3CzBPz**	**2CzBPz**
Formula	$C_{52}H_{32}N_6$	$C_{52}H_{33}N_5$	$C_{52}H_{34}N_4$
Formula weight	740.83	727.83	714.83
Crystal colour, habit	Yellow plate	Yellow prism	Colorless prism
Crystal dimensions (mm^3)	0.10×0.10×0.01	0.13×0.10×0.06	0.17×0.15×0.13
Temperature (K)	125	173	173
Space group	$P\bar{1}$	$P\bar{1}$	$C2/c$
a (Å)	8.9357(3)	9.3062(4)	15.5941(5)
b (Å)	13.9253(6)	9.5819(4)	11.0149(4)
c (Å)	30.4425(12)	23.3719(10)	22.1871(7)
α (°)	78.435(3)	101.559(3)	90
β (°)	86.435(3)	90.366(4)	102.993(3)
γ (°)	85.027(3)	110.580(4)	90
Volume ($Å^3$)	3693.3(3)	1904.80(15)	3713.4(2)
Z	4	2	4

ρ_{calcd} (g cm^{-3})	1.332	1.269	1.279
μ (mm^{-1})	0.621	0.075	0.075
F(000)	1544	760	1496
Reflections collected	51252	25388	24092
independent reflections (R_{int})	19292 (0.1466)	8408 (0.0438)	4378 (0.0276)
Parameters, restraints	1046, 0	514, 36	308, 0
R_1 [I>2σ(I)]	0.1277	0.0550	0.0403
wR_2 (all data)	0.4206	0.1333	0.1046
GoF on F^2	1.606	1.028	1.069
Largest peak/hole [e/Å^3]	0.794 / -0.682	0.279 / -0.263	0.231 / -0.214

Solvatochromic Experiments

Lippert-Mataga Model

The Lippert-Mataga model, which relates the Stokes shift to the solvent polarity factor *f*, can be estimated from the following equation: $hc(v_{ab} - v_{PL}) = hc(v_{ab}^0 - v_{PL}^0) - \frac{2(\mu_e - \mu_g)^2}{a^3} f(\varepsilon, n)$,

where *f* is the orientational polarizability of the solvent; $v_a - v_f$ corresponds to the Stokes shifts when *f* is zero; μ_e is the excited-state dipole moment; μ_g is the ground-state dipole moment; a is the solvent cavity (Onsager) radius derived from Avogadro's number (N), the molecular weight (M), and the density (d = 1.0 g/cm^3); ϵ and n are the solvent dielectric and the solvent refractive index, respectively; $f(\varepsilon, n)$ and a can be calculated, respectively, as follows:

$$f(\varepsilon, n) = \frac{\varepsilon - 1}{2\varepsilon - 1} - \frac{n^2 - 1}{2n^2 + 1}, a = \left(\frac{3M}{4n\pi d}\right)^{1/3}$$

Table **S2**. Detailed solvatochromic investigations of absorption and emission.

Solvents	$f(\varepsilon, n)$	**4CPyz**			**3CzBPz**			**2CzBPz**		
		λ_{ab}	λ_{PL}	$v_{ab} - v_{PL}$	λ_{ab}	λ_{PL}	$v_{ab} - v_{PL}$	λ_{ab}	λ_{PL}	$v_{ab} - v_{PL}$
		nm	**nm**	**cm^{-1}**	**nm**	**nm**	**cm^{-1}**	**nm**	**nm**	**cm^{-1}**
Cyclohexane	1E-4	424	451	1356	407	435	1582	388	433	2678

Toluene	0.014	427	460	1880	403	444	2291	388	436	2837
Triethylamine	0.047	423	452	1506	403	436	1878	387	436	2904
Diethyl ether	0.167	421	456	1791	401	442	2313	388	435	2785
Ethyl acetate	0.199	409	476	3175	399	449	2791	386	439	3128
THF	0.209	412	474	3382	397	450	2967	385	438	3143
Acetone	0.305	404	486	4115	393	461	3753	378	445	3983
Acetonitrile	0.279	399	494	4820	392	479	4633	380	454	4289
Methanol	0.308	412	520	5159	398	511	5556	384	490	5634

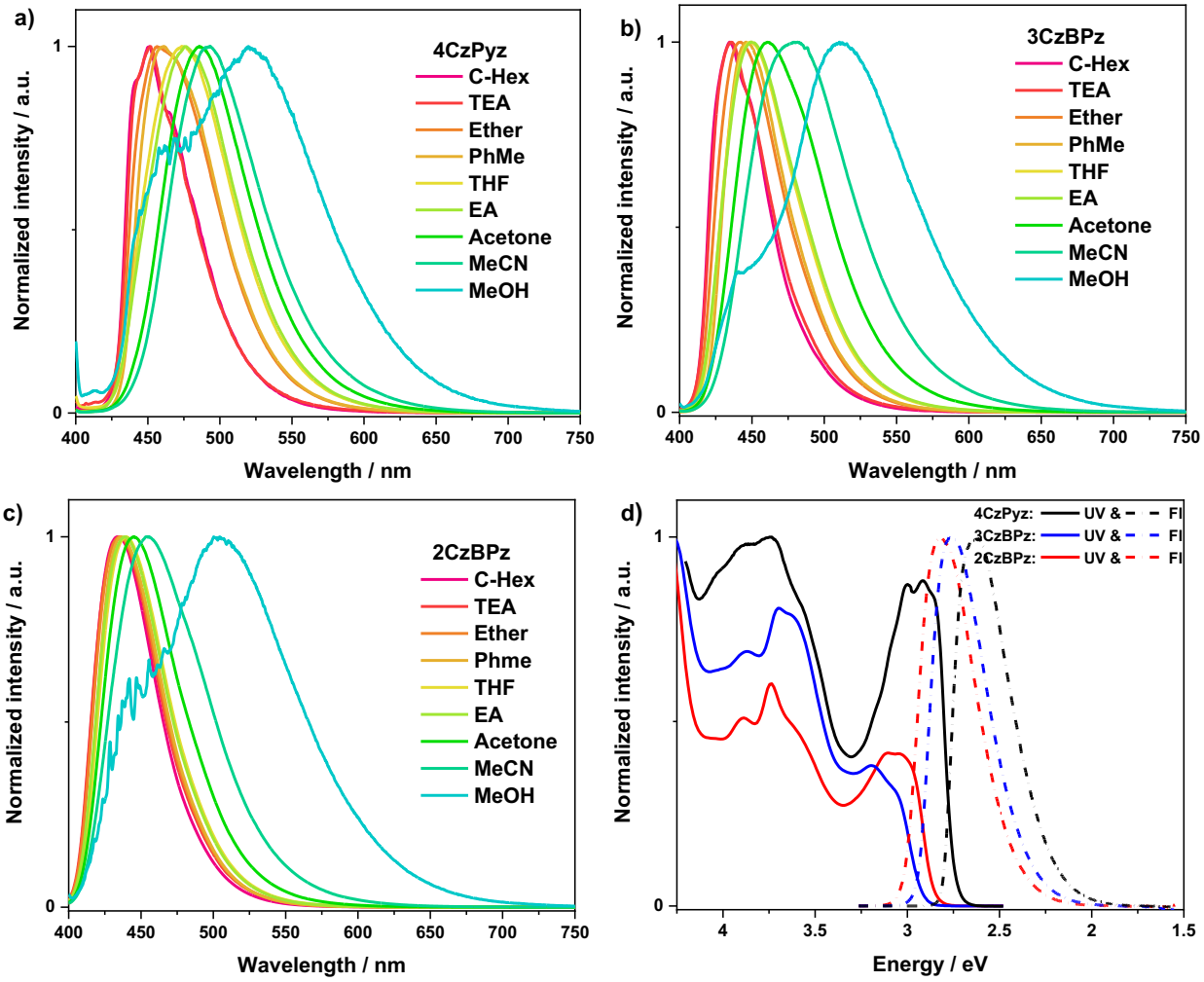

Figure **S5**. Solvatochromic PL spectra of a) **4CzPyz**, b) **3CzBPz**, and c) **2CzBPz** (λ_{exc}: 380 nm), and d) normalized UV-vis and fluorescence spectra in toluene for three emitters (λ_{exc} = 360 nm).

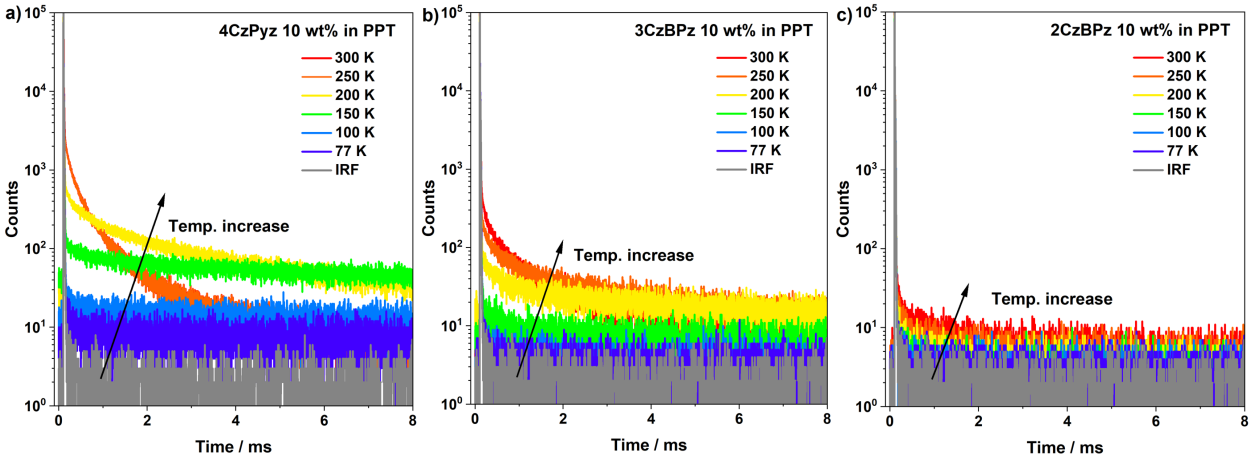

Figure **S6**. Temperature-dependent transient PL decay curves of a) **4CzPyz**, b) **3CzBPz**, and c) **2CzBPz** in 10 wt% doped PPT film (λ_{exc} = 378 nm).

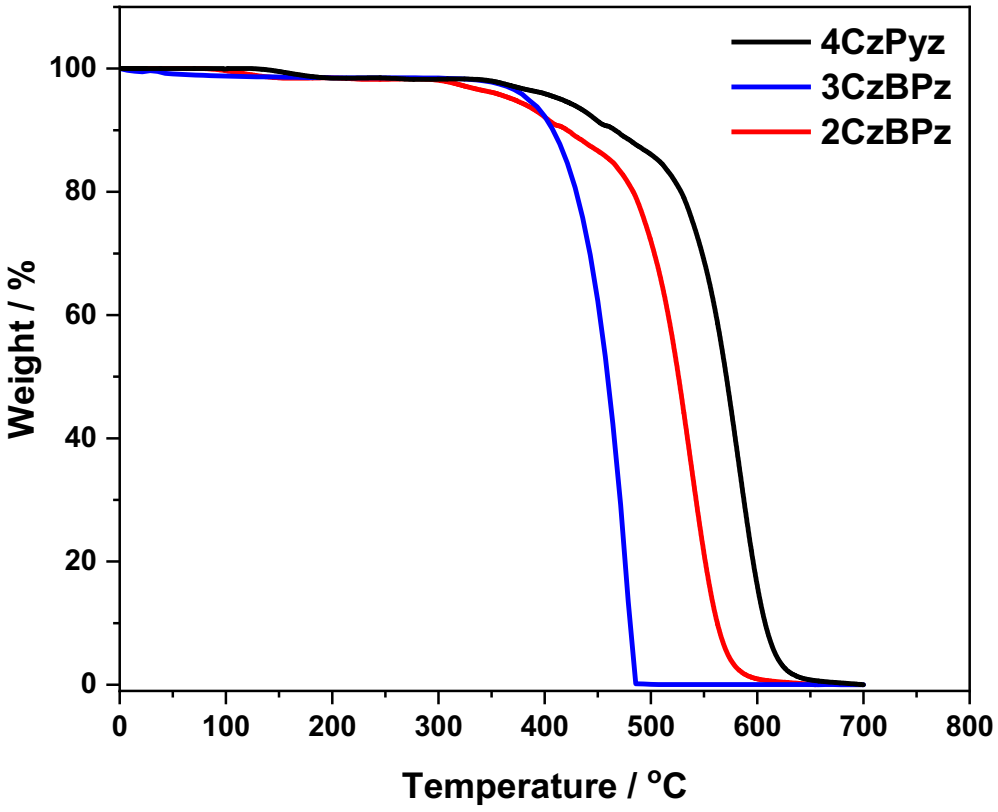

Figure **S7**. Thermogravimetry analysis of **4CzPyz**, **3CzBPz** and **2CzBPz** under N_2 flow (30 mL/min), heating rate: 10 °C/min.

Device fabrication and testing

OLEDs were fabricated using pre-cleaned indium-tin-oxide (ITO) coated glass substrates with ITO thickness of 90 nm. The OLEDs have a pixel area of 2 mm^2. The small molecule and cathode layers were thermally evaporated using an Angstrom deposition chamber at 10^{-7} mbar at 0.3 A/s or 0.6 A/s for organic layers and 1 A/s for the cathode. OLED testing was performed using a sourcemeter (Keithey 2400) and

photodiode, and data analyzed assuming Lambertian emission. Eletroluminescence spectra were collected using a spectrograph (MS125, Oriel) coupled to a CCD camera (DV420-BU, Andor).

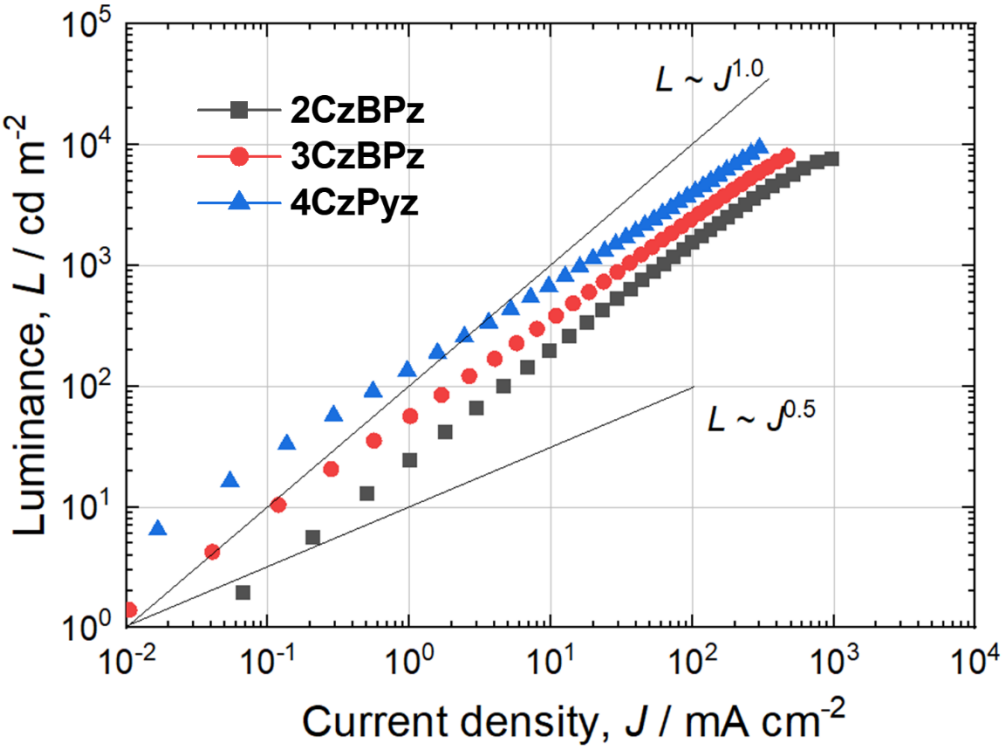

Figure **S8**. Current density- -luminance characteristics of **4CzPyz**, **3CzBPz**, and **2CzBPz**.

Table **S3**. Device performance comparison of **4CzPyz** and selected pyrazine/pyrimidine based blue TADF emitters

Compound	ΔE_{ST}/ eV	V_{on} / V	λ_{EL} / nm	CIE	EQE_{max}	EQE_{100}	EQE_{1000}	Lum_{max} / cd m^{-2}	ref
4CzPyz	0.23	3.0	486	(0.20, 0.39)	24.1%	6.8%	2.6%	11 000	This work
DTCz-Pz	0.27	3.5	460	(0.15, 0.16)	11.6%	4.5%	2.5%	6 900	[21]
2TCzPZCN	0.16	3.9	480	(0.15, 0.26)	12.2%	3.0%	N.A.	6 260	[22]
BFCZPZ2	0.31	3.4	464	(0.15, 0.16)	21.3%	9.1%	5.1%	4 994	[23]
BTCZPZ2	0.31	3.2	468	(0.15, 0.18)	19.7%	9.5%	5.8%	15 000	[23]
CZ9CZPZ	0.31	3.2	468	(0.16, 0.20)	20.0%	10.0%	6.0%	9 930	[23]
3CbzPYR	0.32	4.0	473	(0.16, 0.23)	19.7%	8.8%	4.5%	8 800	[24]
1MPA	0.22	3.2	479	(0.16, 0.21)	14.9%	6.8%	2.9%	8 450	[25]

Table **S4**. Device performance comparison of **3CzBPZ** and blue HLCT emitters based OLEDs

Compound	V_{on} / V	λ_{EL} / nm	CIE	EQE_{max}	EQE_{100}	EQE_{1000}	Lum_{max} / cd m^{-2}	ref
3CzBPz	3.1	464	(0.16, 0.21)	9.6%	3.0%	2.0%	15 000	This work
DTPPI	3.0	462	(0.15, 0.16)	4.2%	N.A.	3.5%	12 355	[26]
TBPMCN	4.5	460	(0.16, 0.16)	7.8%	N.A.	5.5%	5 000	[27]
2TriPE-BPI-MCN	3.8	450	(0.15, 0.15)	4.6%	4.5%	4.4%	6 130	[28]
2CzPh-CNNPI	3.1	440	(0.15, 0.10)	9.0%	4.1%	3.1%	3 650	[29]
TPP-TXO2	3.1	450	(0.15, 0.07)	10.5%	5.6%	4.6%	10 000	[30]
Cz-TPB	3.2	452	(0.15, 0.10)	4.3%	3.3%	2.0%	3 300	[31]

PyPPA	2.8	464	(0.14, 0.13)	8.5%	8.0%	5.5%	30 300	[32]

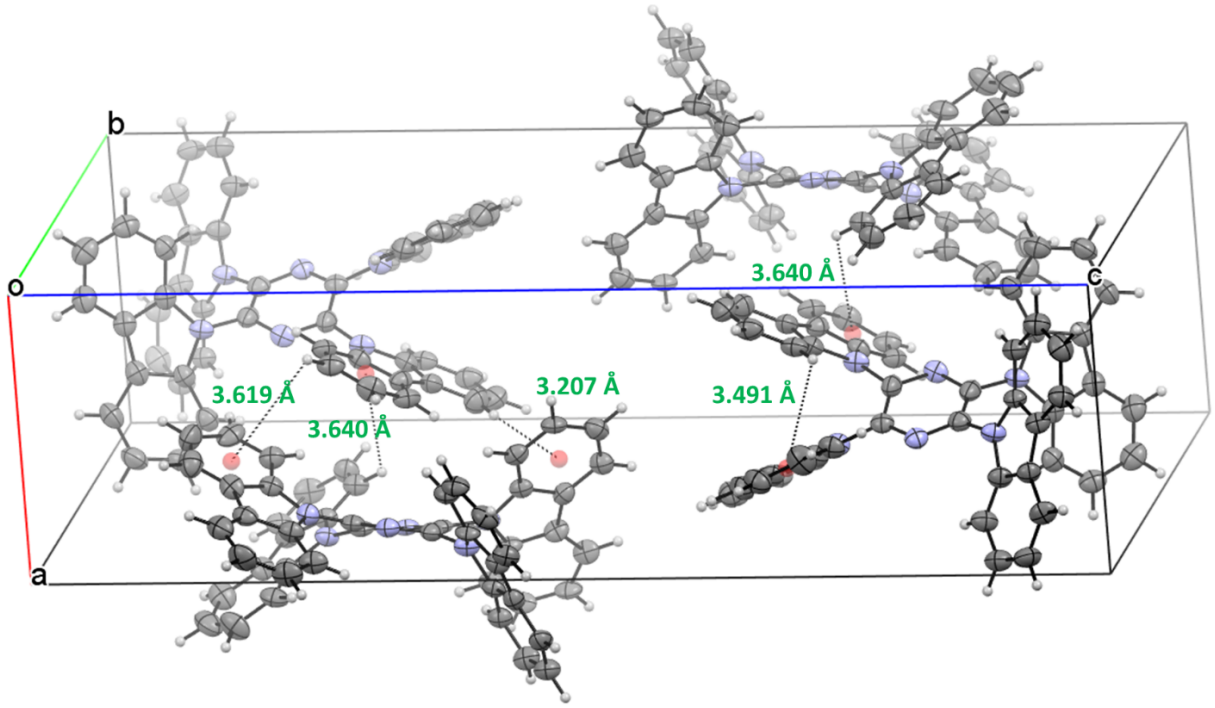

Figure **S9**. Packing view of the structure of **4CzPyz** .

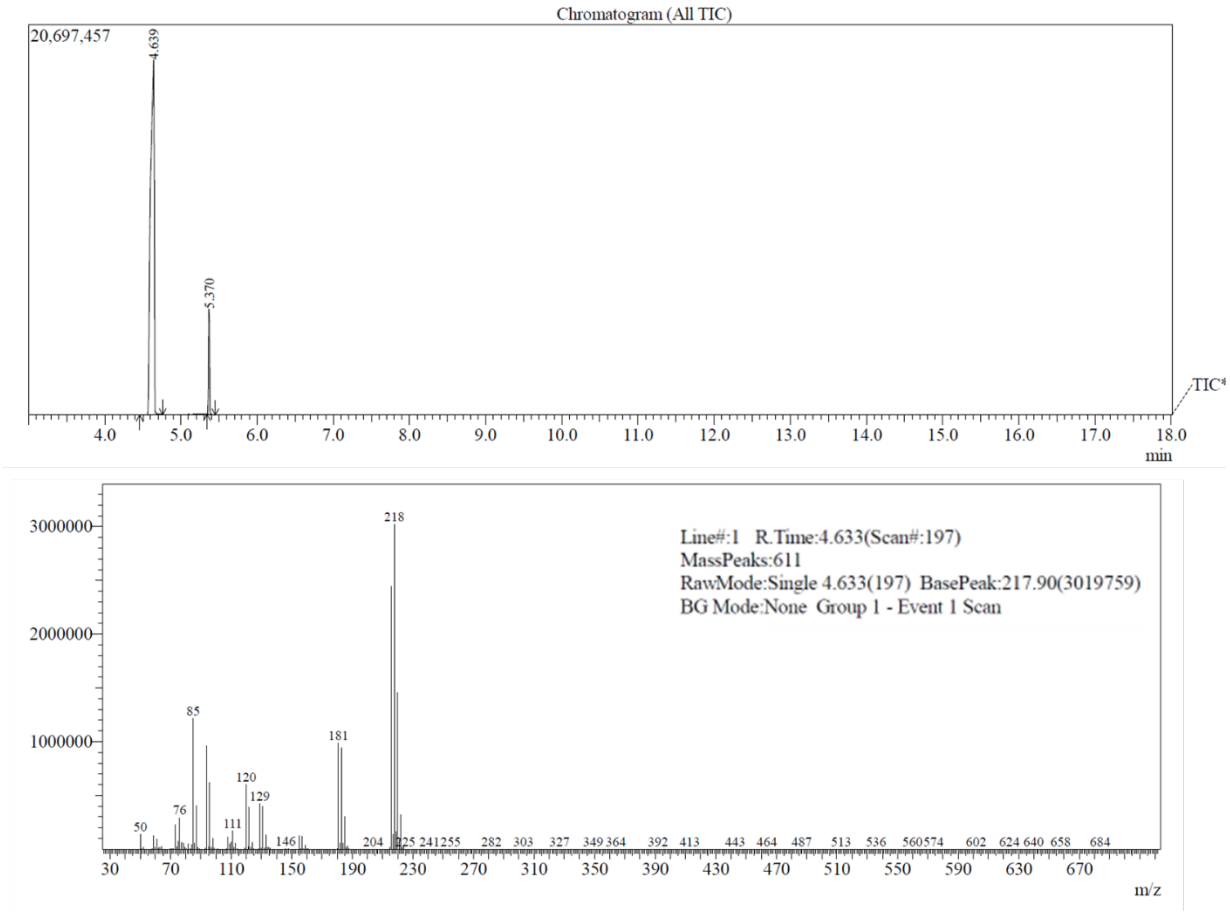

Figure **S10**. LRMS of **4ClPz**.

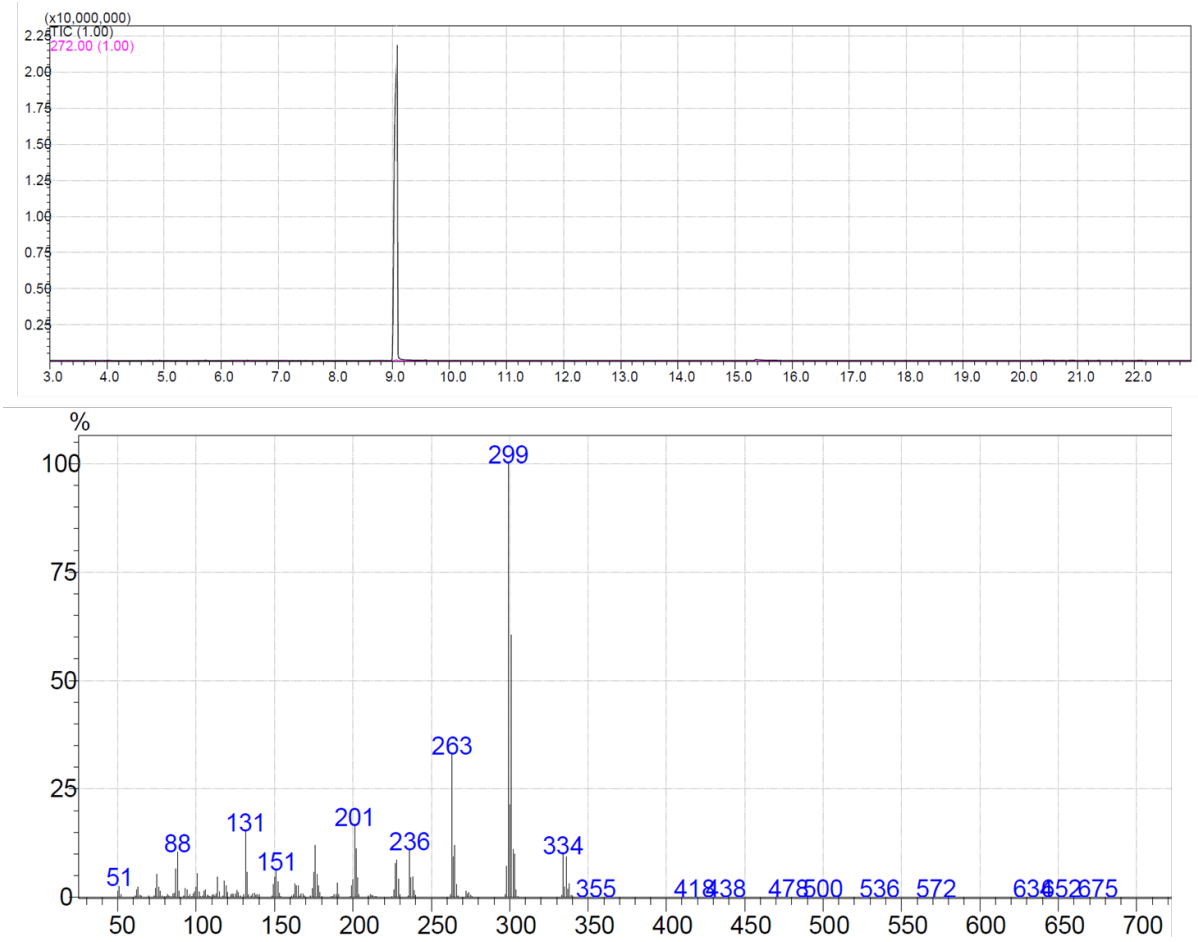

Figure **S11**. LRMS of **3ClBPz**.

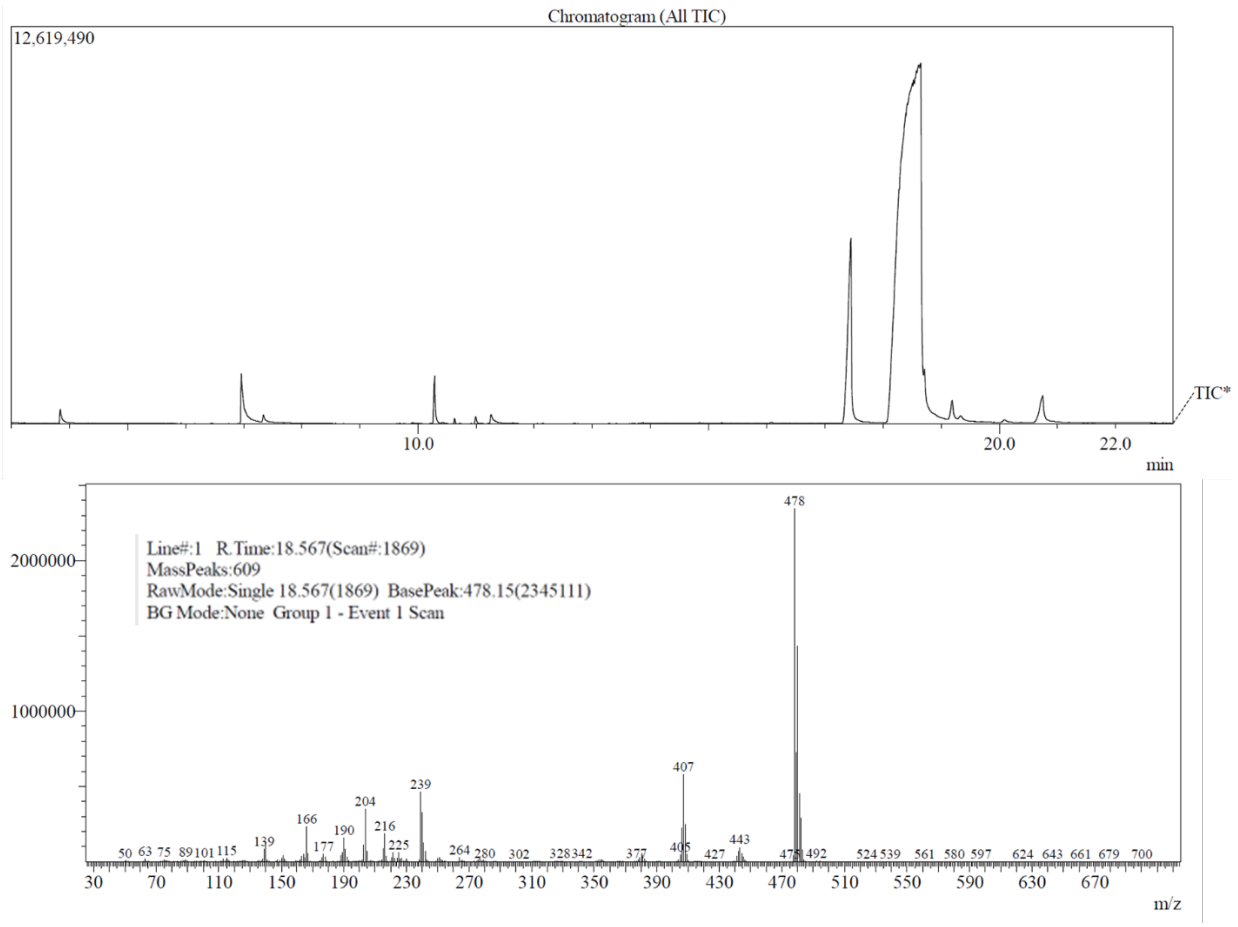

Figure **S12**. LRMS of **2Cz2ClPz**.

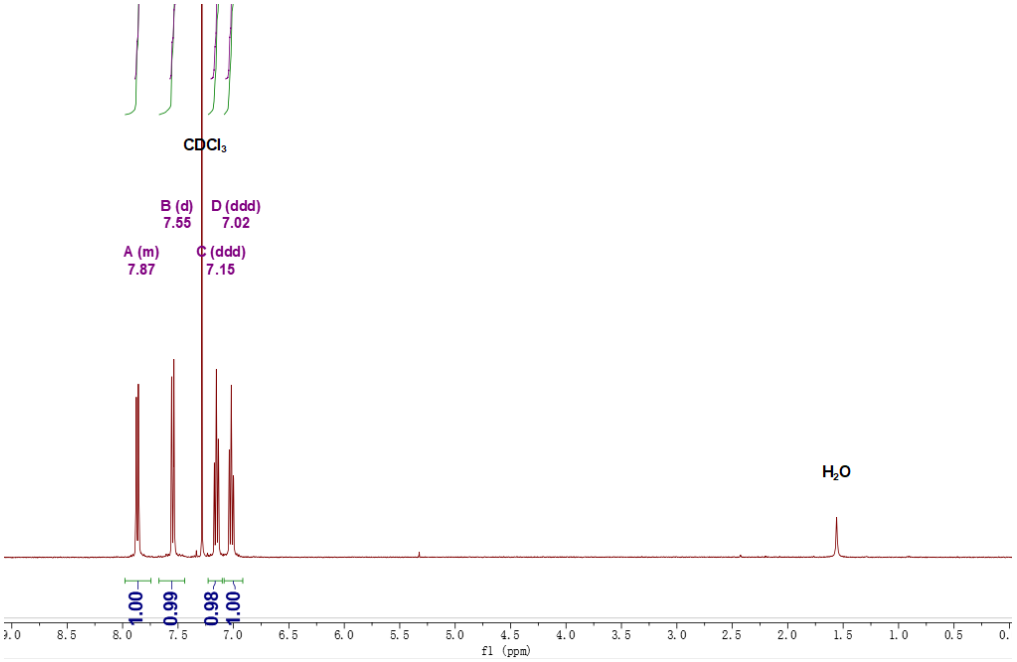

Figure **S13**. ^{1}H NMR of **4CzPyz** in $CDCl_3$

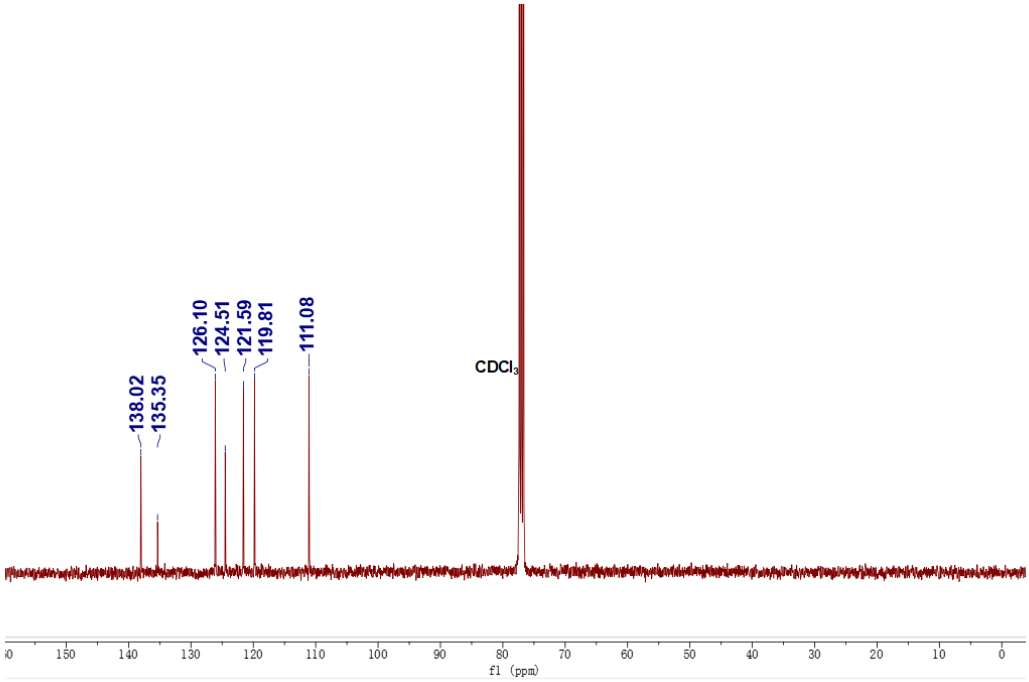

Figure **S14**. ^{13}C NMR of **4CzPyz** in $CDCl_3$

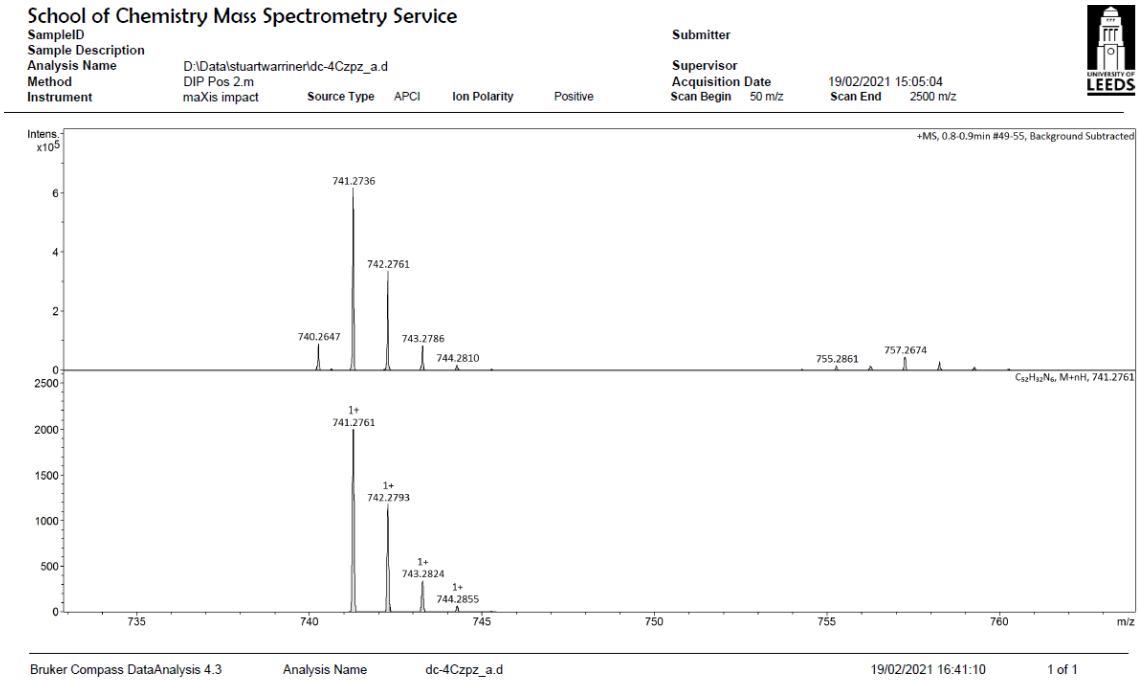

Figure **S15**. HRMS of **4CzPyz**

Elemental Analysis Service Request Form

Researcher name Dongyang Chen

Researcher email dc217@st-andrews.ac.uk

NOTE: Please submit ca. 10 mg of sample

Sample reference number	dc-II212
Name of Compound	4CzPz
Molecular formula	C52H32N6
Stability	stable
Hazards	low hazard
Other Remarks	

Analysis type:

Single ☐ **Duplicate**√☐ **Triplicate**☐

Analysis Result:

Element	Expected %	Found (1)	Found (2)	Found (3)
Carbon	84.30	84.89	84.30	
Hydrogen	4.35	4.24	4.28	
Nitrogen	11.34	11.11	11.02	
Oxygen				

Authorising Signature:

Date completed	26.02.21
Signature	JPC
comments	

Figure **S16**. Elemental analysis of **4CzPyz**

SHIMADZU LabSolutions **Analysis Report**

<Sample Information>

Sample Name	: 4CzPz 95 methanol		
Sample ID	:		
Data Filename	: 4CzPz4tCzPz2_28092020_4CzPz 95 methanol_003.lcd		
Method Filename	: 95% Methanol 5 Water 20 mins.lcm		
Batch Filename	: 4CzPz4tCzPz2.lcb		
Vial #	: 1-11	Sample Type	: Unknown
Injection Volume	: 10 uL		
Date Acquired	: 28/09/2020 12:25:52	Acquired by	: System Administrator
Date Processed	: 28/09/2020 12:50:55	Processed by	: System Administrator

<Chromatogram>

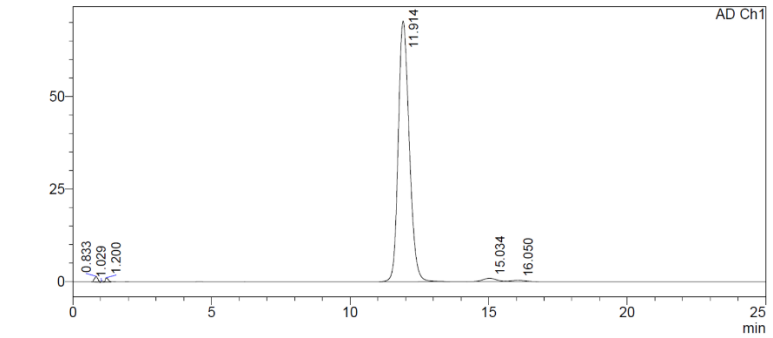

<Peak Table>

Peak#	Ret. Time	Area	Height	Conc.	Unit	Area%
1	0.837	11668	1472	0.000		0.592
2	1.203	8161	1039	0.000	mg/L	0.414
3	11.915	1930492	70276	0.000	mg/L	97.884
4	15.036	21908	763	0.000		1.111
Total		1972230	73551			100.000

Figure **S17**. HPLC report of **4CzPyz**

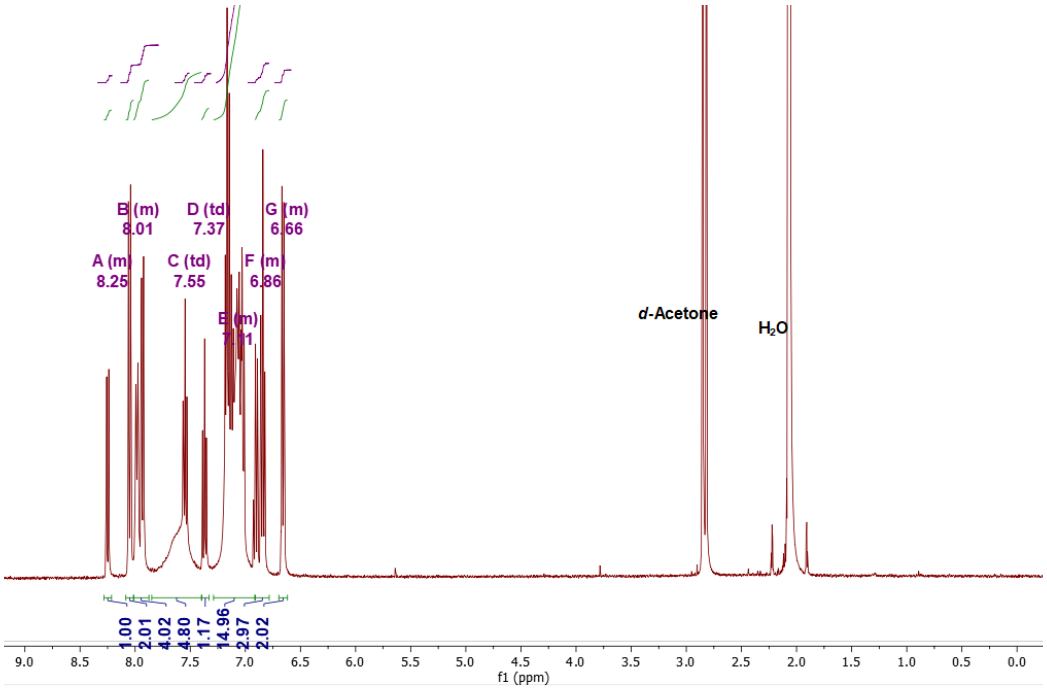

Figure **S18**. [1]H NMR of **3CzBPz** in *d*-Acetone

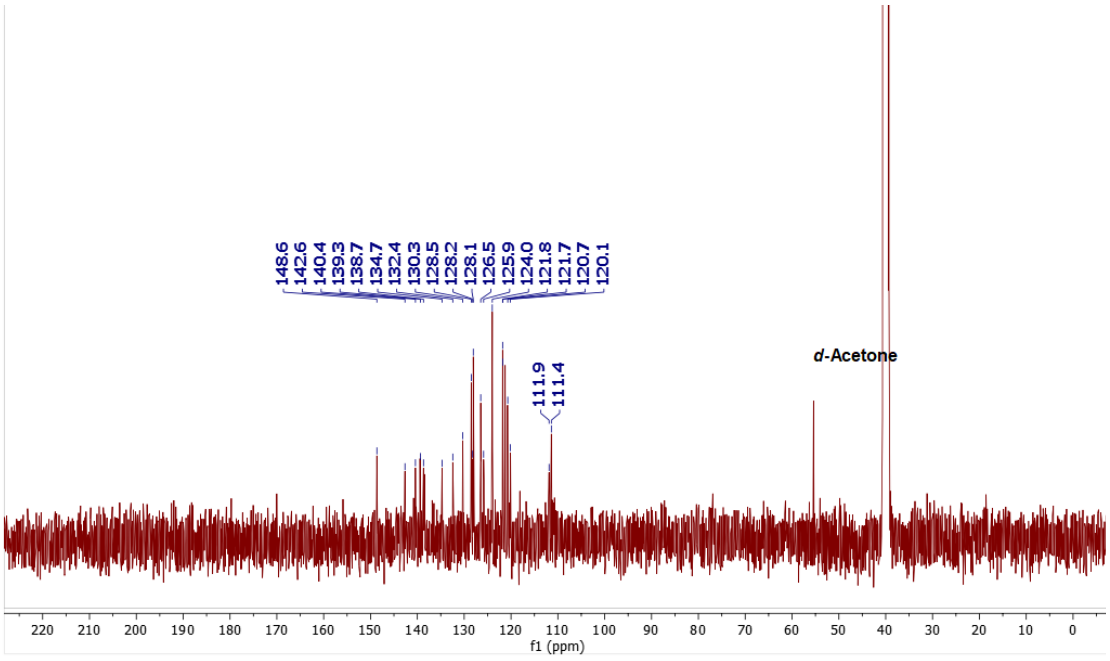

Figure **S19**. [13]C NMR of **3CzBPz** in *d*-Acetone

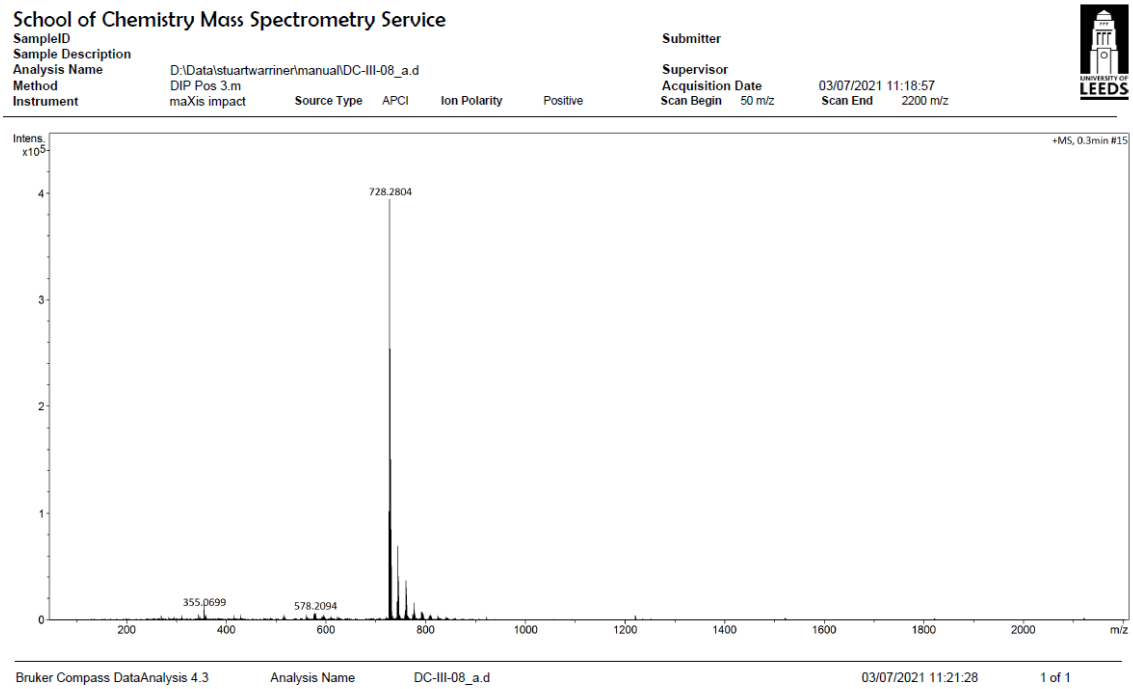

Figure **S20**. HRMS of **3CzBPz**

Elemental Analysis Service Request Form

Researcher name Dongyang Chen

Researcher email dc217@st-andrews.ac.uk

NOTE: Please submit ca. 10 mg of sample

Sample reference number	dc-III07
Name of Compound	3CzBPz
Molecular formula	C52H33N5
Stability	stable
Hazards	low hazard
Other Remarks	

Analysis type:

Single ☐ **Duplicate**√☐ **Triplicate**☐

Analysis Result:

Element	Expected %	Found (1)	Found (2)	Found (3)
Carbon	85.81	85.53	85.60	
Hydrogen	4.57	4.66	4.66	
Nitrogen	9.62	9.46	9.47	
Oxygen				

Authorising Signature:

Date completed	21.05.21
Signature	J-P Li
comments	

Figure **S21**. Elemental analysis of **3CzBPz**

HPLC Trace Report17Apr2021

<Sample Information>

Sample Name	: 3CzBPz		
Sample ID	:		
Method Filename	: 98% Methanol 2 Water 20 mins.lcm		
Batch Filename	: 3CzBPz 2CzBPz 98 MeOH.lcb		
Vial #	: 1-37	Sample Type	: Unknown
Injection Volume	: 50 uL		
Date Acquired	: 12/04/2021 14:21:28	Acquired by	: System Administrator
Date Processed	: 12/04/2021 14:46:31	Processed by	: System Administrator

<Chromatogram>

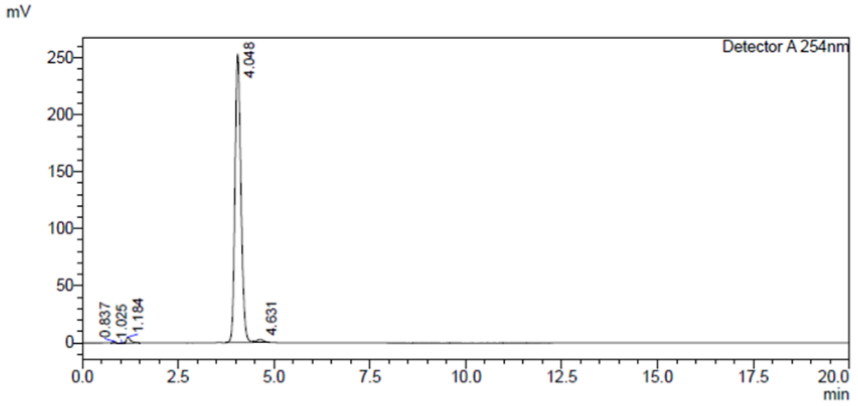

<Peak Table>

Detector A 254nm

Peak#	Ret. Time	Area	Height	Area%	Area/Height	Width at 5% Height
1	0.837	5330	1436	0.189	3.711	0.127
2	1.025	3572	443	0.127	8.072	--
3	1.184	38627	5250	1.372	7.358	--
4	4.048	2734332	252217	97.897	10.841	0.366
5	4.631	33933	2697	1.205	12.582	--
Total		2815793	262042	100.000		

Figure **S22**. HPLC of **3CzBPz**

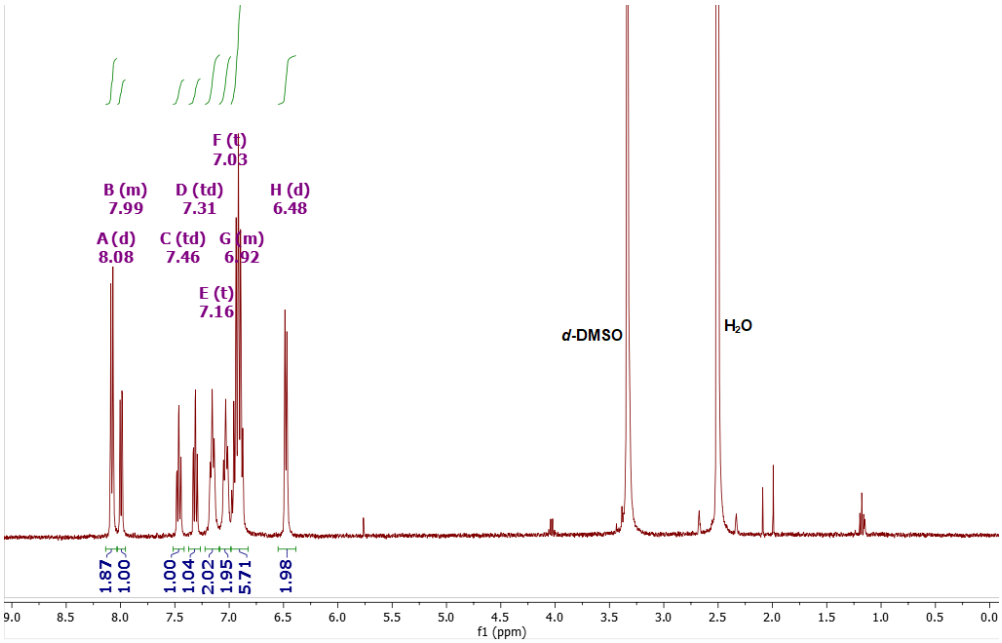

Figure **S23**. ^{1}H NMR of **2CzBPz** in d_6-DMSO

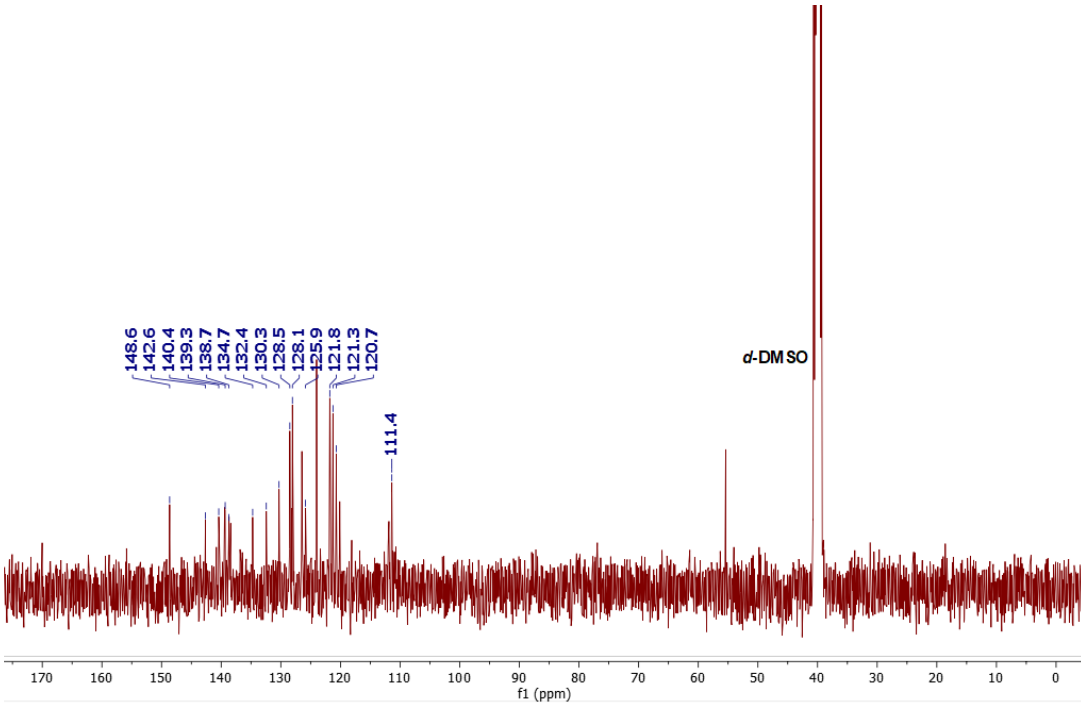

Figure **S24**. ^{13}C NMR of **2CzBPz** in d_6-DMSO

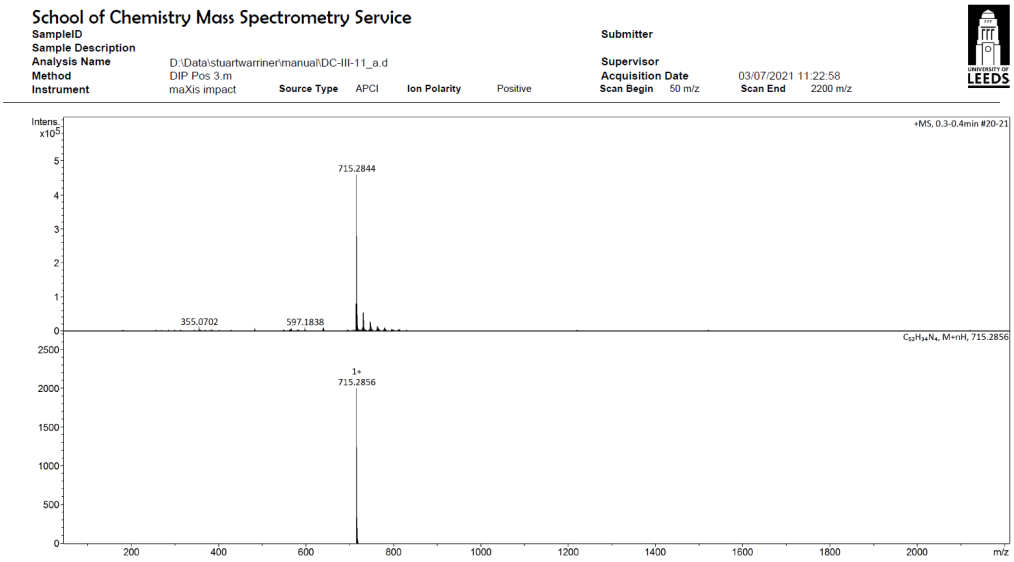

Figure **S25**. HRMS of **2CzBPz**

Elemental Analysis Service Request Form

Researcher name Dongyang Chen

Researcher email dc217@st-andrews.ac.uk

NOTE: Please submit ca. 10 mg of sample

Sample reference number	dc-III12
Name of Compound	2CzBPz
Molecular formula	C52H34N4
Stability	stable
Hazards	low hazard
Other Remarks	

Analysis type:

Single ☐ **Duplicate**√☐ **Triplicate**☐

Analysis Result:

Element	Expected %	Found (1)	Found (2)	Found (3)
Carbon	87.37	87.54	89.44	
Hydrogen	4.79	4.89	4.97	
Nitrogen	7.84	7.78	7.93	
Oxygen				

Authorising Signature:

Date completed	21.05.21
Signature	J-Pc
comments	

Figure **S26**. Elemental analysis of **2CzBPz**

HPLC Trace Report17Apr2021

<Sample Information>

Sample Name	: 3CzBPz		
Sample ID	:		
Method Filename	: 98% Methanol 2 Water 20 mins.lcm		
Batch Filename	: 3CzBPz 2CzBPz 98 MeOH.lcb		
Vial #	: 1-37	Sample Type	: Unknown
Injection Volume	: 50 uL		
Date Acquired	: 12/04/2021 14:21:28	Acquired by	: System Administrator
Date Processed	: 12/04/2021 14:46:31	Processed by	: System Administrator

<Chromatogram>

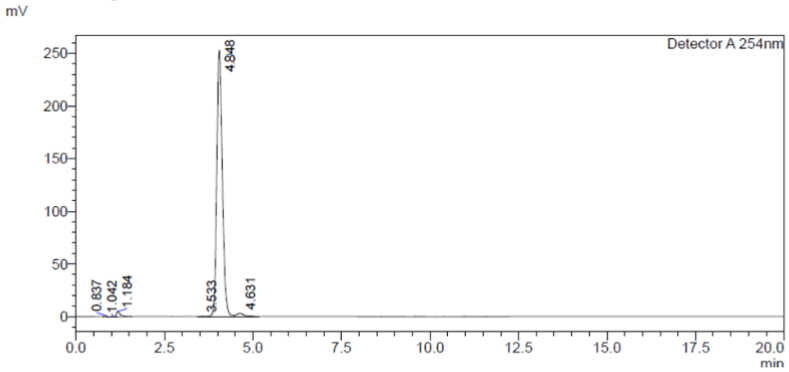

<Peak Table>

Detector A 254nm

Peak#	Ret. Time	Area	Height	Area%	Area/Height	Width at 5% Height
1	0.837	5342	1437	0.188	3.718	0.127
2	1.042	3488	485	0.123	7.191	--
3	1.184	40717	5299	1.432	7.684	--
4	3.533	2504	208	0.088	12.016	--
5	4.048	2744564	252439	98.523	10.872	0.367
6	4.631	46830	3059	1.647	15.311	--
Total		2843444	262927	100.000		

Figure **S27**. HPLC report of **2CzBPz**

References

(1) Fleischhauer, J.; Zahn, S.; Beckert, R.; Grummt, U. W.; Birckner, E.; Görls, H. A Way to Stable, Highly Emissive Fluorubine Dyes: Tuning the Electronic Properties of Azaderivatives of Pentacene by Introducing Substituted Pyrazines. *Chemistry - A European Journal* **2012**, *18* (15), 4549–4557. https://doi.org/10.1002/chem.201103350.

(2) Salah, L.; Etherington, M. K.; Shuaib, A.; Danos, A.; Nazeer, A. A.; Ghazal, B.; Prlj, A.; Turley, A. T.; Mallick, A.; McGonigal, P. R.; Curchod, B. F. E.; Monkman, A. P.; Makhseed, S. Suppressing Dimer Formation by Increasing Conformational Freedom in Multi-Carbazole Thermally Activated Delayed Fluorescence Emitters. *Journal of Materials Chemistry C* **2021**, *9* (1), 189–198. https://doi.org/10.1039/d0tc04222f.

(3) Adamo, C.; Barone, V. Toward Reliable Density Functional Methods without Adjustable Parameters: The PBE0 Model. *Journal of Chemical Physics* **1999**, *110* (13), 6158–6170. https://doi.org/10.1063/1.478522.

(4) Pople, J. A.; Binkley, J. S.; Seeger, R. Theoretical Models Incorporating Electron Correlation. *International Journal of Quantum Chemistry* **1976**, *10*, 1–19. https://doi.org/10.1002/qua.560100802.

(5) Hirata, S.; Head-Gordon, M. Time-Dependent Density Functional Theory within the Tamm–Dancoff Approximation. *Chem. Phys. Lett.* **1999**, *314*, 291–299.

(6) Grimme, S. Density Functional Calculations with Configuration Interaction for the Excited States of Molecules. *Chem. Phys. Lett.* **1996**, *259*, 128–137.

(7) Gao, X.; Bai, S.; Fazzi, D.; Niehaus, T.; Barbatti, M.; Thiel, W. Evaluation of Spin-Orbit Couplings with Linear-Response Time-Dependent Density Functional Methods. *Journal of Chemical Theory and Computation* **2017**, *13* (2), 515–524. https://doi.org/10.1021/acs.jctc.6b00915.

(8) Frisch, M. J.; Trucks, G. W.; Schlegel, H. B.; Scuseria, G. E.; Robb, M. A.; Cheeseman, J. R.; Scalmani, G.; Barone, V.; Mennucci, B.; Petersson, G. A.; Nakatsuji, H.; Caricato, M.; Li, X.; Hratchian, H. P.; Izmaylov, A. F.; Bloino, J.; Zheng, G.; Sonnenberg, J. L.; Had, M.; Fox, D. J. Gaussian 09, Revis. D.01. Wallingford, CT. 2009.

(9) Moral, M.; Muccioli, L.; Son, W.-J.; Olivier, Y.; Sancho-García, J. C. Theoretical Rationalization of the Singlet–Triplet Gap in OLEDs Materials: Impact of Charge-Transfer Character. *J. Chem. Theory Comput.* **2015**, *11* (1), 168–177.

(10) GaussView, Version 6.1, Roy Dennington, Todd A. Keith, and John M. Millam, Semichem Inc., Shawnee Mission, KS, 2016.

(11) Demas, J. N.; Crosby, G. A. The Measurement of Photolumineseence Quantum Yields. A Review. *The Journal of Physical Chemistry* **1971**, *75* (8), 991–1024. https://doi.org/10.1021/j100678a001.

(12) Melhuish, W. H. Quantum Efficiencies of Fluorescence of Organic Substan Ces: Effect of Solvent and Concentration of the Fluorescent Solute. *Journal of Physical Chemistry* **1961**, *65* (2), 229–235. https://doi.org/10.1021/j100820a009.

(13) Greenham, N. C.; Samuel, I. D. W.; Hayes, G. R.; Phillips, R. T.; Kessener, Y. A. R. R.; Moratti, S. C.; Holmes, A. B.; Friend, R. H. Measurement of Absolute Photoluminescence Quantum Efficiencies in Conjugated

Polymers. *Chem Phys Lett* **1995**, *241* (1), 89–96. https://doi.org/https://doi.org/10.1016/0009-2614(95)00584-Q.

(14) Pavlishchuk, V. V.; Addison, A. W. Conversion Constants for Redox Potentials Measured versus Different Reference Electrodes in Acetonitrile Solutions at 25°C. *Inorganica Chimica Acta* **2000**, *298*, 97–102. https://doi.org/10.1016/S0020-1693(99)00407-7.

(15) CrystalClear-SM Expert v. 2.1; . Rigaku Americas, Rigaku Americas, The Woodlands, Texas, USA and Rigaku Corporation, Tokyo, Japan,. 2015.

(16) CrysAlisPro v1.171.41.93a.; Rigaku Oxford Diffraction, Rigaku Corporation,: Oxford, U.K., 2020.

(17) Burla, M. C.; Caliandro, R.; Camalli, M.; Carrozzini, B.; Cascarano, G. L.; Giacovazzo, C.; Mallamo, M.; Mazzone, A.; Polidori, G.; Spagna, R. A New Package for Crystal Structure Determination and Refinement. *J. Appl. Cryst.* **2012**, *45*, 357–361.

(18) Sheldrick, G. M. SHELXT – Integrated Space-Group and Crystal Structure Determination. *Acta Crystallogr., Sect. A: Found. Adv.* **2015**, *71*, 3–8. https://doi.org/10.1107/S2053273314026370.

(19) Sheldrick, G. M. Crystal Structure Refinement with SHELXL. *Acta Crystallogr. Sect. C Struct. Chem.* **2015**, *71* (1), 3–8. https://doi.org/10.1107/S2053229614024218.

(20) Dolomanov, O. V; Bourhis, L. J.; Gildea, R. J.; Howard, J. A. K.; Puschmann, H. OLEX2: A Complete Structure Solution, Refinement and Analysis Program. *Journal of Applied Crystallography* **2009**, *42*, 339–341. https://doi.org/10.1107/S0021889808042726.

(21) Rajamalli, P.; Chen, D.; Suresh, S. M.; Tsuchiya, Y.; Adachi, C.; Zysman-Colman, E. Planar and Rigid Pyrazine-Based TADF Emitter for Deep Blue Bright Organic Light-Emitting Diodes. *European Journal of Organic Chemistry* **2021**, *2021* (16), 2285–2293. https://doi.org/10.1002/ejoc.202100086.

(22) Liu, J.; Zhou, K.; Wang, D.; Deng, C.; Duan, K.; Ai, Q.; Zhang, Q. Pyrazine-Based Blue Thermally Activated Delayed Fluorescence Materials: Combine Small Singlet-Triplet Splitting with Large Fluorescence Rate. *Frontiers in Chemistry* **2019**, *7*, 1–9.

(23) Cai, M.; Auffray, M.; Zhang, D.; Zhang, Y.; Nagata, R.; Lin, Z.; Tang, X.; Chan, C. Y.; Lee, Y. T.; Huang, T.; Song, X.; Tsuchiya, Y.; Adachi, C.; Duan, L. Enhancing Spin-Orbital Coupling in Deep-Blue/Blue TADF Emitters by Minimizing the Distance from the Heteroatoms in Donors to Acceptors. *Chemical Engineering Journal* **2021**, *420* (P2), 127591. https://doi.org/10.1016/j.cej.2020.127591.

(24) Serevičius, T.; Dodonova, J.; Skaisgiris, R.; Banevičius, D.; Kazlauskas, K.; Juršėnas, S.; Tumkevičius, S. Optimization of the Carbazole-Pyrimidine Linking Pattern for Achieving Efficient TADF. *Journal of Materials Chemistry C* **2020**, *8* (32), 11192–11200. https://doi.org/10.1039/d0tc02194f.

(25) Ko, A.; Strohriegl, P. Low Efficiency Roll-off Blue TADF OLEDs Triplet Energy Host †. *Journal of Materials Chemistry C* **2021**, *9*, 17471–17482. https://doi.org/10.1039/d1tc03598c.

(26) Zhong, Z.; Zhu, X.; Wang, X.; Zheng, Y.; Geng, S.; Zhou, Z.; Feng, X.; Zhao, Z.; Lu, H. High Steric-Hindrance Windmill-Type Molecules for Efficient Ultraviolet to Pure-Blue. *Adv. Funct. Mater.* **2022**, *32*, 2112969. https://doi.org/https://doi.org/10.1002/adfm.202112969.

(27) Zhang, S.; Yao, L.; Peng, Q.; Li, W.; Pan, Y.; Xiao, R.; Gao, Y.; Gu, C.; Wang, Z.; Lu, P.; Li, F.; Su, S.; Yang, B.; Ma, Y. Achieving a Signifi Cantly Increased Effi Ciency in Nondoped Pure Blue Fluorescent OLED : A Quasi-Equivalent Hybridized Excited State. *Adv. Funct. Mater.* **2015**, *25*, 1755–1762. https://doi.org/10.1002/adfm.201404260.

(28) Zhang, H.; Li, A.; Li, G.; Li, B.; Wang, Z.; Xu, S.; Xu, W.; Tang, B. Z. Achievement of High-Performance Nondoped Blue OLEDs Based on AIEgens via Construction of Effective High-Lying Charge-Transfer State. *Adv Opt Mater* **2020**, *8* (14), 1902195. https://doi.org/https://doi.org/10.1002/adom.201902195.

(29) Zhang, H.; Zhang, B.; Zhang, Y.; Xu, Z.; Wu, H.; Yin, P.-A.; Wang, Z.; Zhao, Z.; Ma, D.; Tang, B. Z. A Multifunctional Blue-Emitting Material Designed via Tuning Distribution of Hybridized Excited-State for High-Performance Blue and Host-Sensitized OLEDs. *Adv Funct Mater* **2020**, *30* (35), 2002323. https://doi.org/https://doi.org/10.1002/adfm.202002323.

(30) Fu, C.; Luo, S.; Li, Z.; Ai, X.; Pang, Z.; Li, C.; Chen, K.; Zhou, L.; Li, F.; Huang, Y.; Lu, Z. Highly Efficient Deep-Blue OLEDs Based on Hybridized Local and Charge-Transfer Emitters Bearing Pyrene as the Structural Unit. *Chemical Communications* **2019**, *55* (44), 6317–6320. https://doi.org/10.1039/c9cc02355k.

(31) Yang, J.; Guo, Q.; Wang, J.; Ren, Z.; Chen, J.; Peng, Q.; Ma, D.; Li, Z. Rational Molecular Design for Efficient Exciton Harvesting, and Deep-Blue OLED Application. *Adv Opt Mater* **2018**, *6* (15), 1800342. https://doi.org/https://doi.org/10.1002/adom.201800342.

(32) Liu, Y.; Liu, H.; Bai, Q.; Du, C.; Shang, A.; Jiang, D.; Tang, X.; Lu, P. Pyrene[4,5- d]Imidazole-Based Derivatives with Hybridized Local and Charge-Transfer State for Highly Efficient Blue and White Organic Light-Emitting Diodes with Low Efficiency Roll-Off. *ACS Applied Materials and Interfaces* **2020**, *12* (14), 16715–16725. https://doi.org/10.1021/acsami.0c01846.